Development of an integrative heat risk index for urban neighbourhoods: Combining T$_{mrt}$ modelling and vulnerability assessment

Wissenschaftliche Arbeit zur Erlangung des Grades

M.Sc. Umweltplanung und Ingenieurökologie

am Wissenschaftszentrum Weihenstephan,
Lehrstuhl für Strategie und Management der Landschaftsentwicklung

Autorin: Sabrina Erlwein
             Kepserstraße 50
             85356 Freising
             s.erlwein@tum.de

Erstprüfer: Prof. Dr. Stephan Pauleit

Betreuung: Prof. Dr, Stephan Pauleit, Teresa Zölch

Ausgabe: 01.06.2016

Abgabe: ………………………

Contents

List of Figures

List of Tables

Acronyms and abbreviations

CDP   city district parts

DEM   digital elevation model

DWD   German Meteorological Service (Deutscher Wetterdienst)

GVF   ground view factor

HVI   heat vulnerability index

MIM   Meteorological Institute Munich

PET   physiological equivalent temperature

RH   relative humidity

SOLWEIG   SOlar and Long Wave Environmental Irradiance Geometry model

SVF   sky view factor

T_{mrt} mean radiant temperature

T_{air} air temperature

UGI   urban green infrastructure

UHI   urban heat island

UN-Habitat   United Nations Human Settlements Programme

ZSK   Centre for Urban Ecology and Climate Adaptation (Zentrum für Stadtnatur und Klimaanpassung)

Abstract

According to current climate projections, heatwaves are expected to rise in duration, frequency and/or intensity. Due to high concentration of vulnerable people and infrastructure, proceeding urbanization and already elevated temperatures in cities due to the urban heat island effect, urban areas are especially threatened. This work presents a spatially explicit heat risk assessment approach for urban areas that combines hazard assessment by modelling of mean radiant temperature (T_{mrt}) with vulnerability analysis. Mean radiant temperature is able to provide information about human thermal comfort for clear, warm summer days. The radiation flux model SOLWEIG, topographical and meteorological input data were used to model the spatio-temporal distribution of T_{mrt} during a chosen heat day for the study site Maxvorstadt in Munich. Nine socio-economic and two physical environment indicators (percentage of trees and proximity to parks) were selected for the vulnerability index. The highest T_{mrt} loads were observable between 2-3 pm, the lowest from 5-6 am. Shadow of buildings and vegetation equally lower T_{mrt}, while a negative linear relationship between tree coverage and T_{mrt} is apparent. Open spaces are hottest during daytime and coolest during nighttime, while the opposite applies to densely tree covered sites. Combination of hazard and vulnerability assessment provide valuable insights for city planners, while availability of spatially more specific data improves assessment results. Further research should investigate the relationship between thermal comfort perceptions and T_{mrt}.

1   Introduction

According to the current projections of average climate change, the frequency of extreme weather events is likely to increase. Heatwaves are expected to rise in duration, frequency and/or intensity (Meehl and Tebaldi, 2004). As regards Germany, almost all weather stations have registered an increasing occurrence of heat waves in July and August over the last hundred years and especially the last decades (Umweltbundesamt, 2005). Moreover, the probability for an extremely hot summer like 2003 has increased by a factor of 20 (Umweltbundesamt, 2005). However, of all natural disasters, heat waves often claim the highest number of fatalities (Gabriel and Endlicher, 2011, Stéphan et al., 2005). The intense heat wave of 2003 is estimated to have caused 70,000 heat-related deaths in Southern and Western Europe (Robine et al., 2007). Studying climate and mortality data of Berlin and Federal State Brandenburg, Gabriel and Endlicher (2011) reported that mortality rates were up to 67.2% higher during extreme heat waves in 1994 and 2006. Doick and colleagues (2013) assume that 8 to 11 extra death occur each day for each degree increase in air temperature during UK summer heatwaves. Scherer et al (2014) suggest that 5 % of all deaths between 2001 and 2010 in Berlin can statistically be related to elevated air temperatures.

Heat stress poses a particular thread to urban regions as these already tend to be warmer than their rural surroundings and are more vulnerable with respect to their population and infrastructure (Geneletti and Zardo, 2016; Scherer et al., 2014, Solecki et al., 2015). Several local factors of urban areas contribute to the urban heat island effect (UHI): Differences in land cover and albedo - more sealed, dark surfaces compared to rural regions -, reduced evapotranspiration (Doick et al., 2013; Oleson et al., 2015), anthropogenic heat emissions (e.g. from traffic and industry) (Wilhelmi et al., 2004), decrease of surface long radiation loss due to urban canyons (Oke, 1992) and heat storage in buildings and sealed roads (Gabriel and Endlicher, 2011) are responsible for rural-urban temperature differences. Since heat stored in the urban fabric throughout daytime is released during the night, UHI intensity is commonly highest during evening and night, counterbalancing nocturnal cooling (Fenner et al., 2014; Scherer et al., 2014). This is especially pronounced during the warmer season: According to Fenner et al. (2014), nocturnal UHI intensity in Berlin was on average about 4 to 5 K during summer days. As thermal and radiative properties differ from site to site, not only one single heat island, but several scattered over the city can be found (Pauleit, 2007; Fenner et al., 2014). Bradford et al., (2015) report that the UHI effect is intensified during extreme heat events.

Today, more than half of the world's population lives in cities, a number that is expected to increase to 69% by 2050 due to the continuing trend towards urbanisation (IPCC, 2014; UN, 2011). Not only are more people exposed to hazards than in rural regions, but they are also

concentrated on less space, increasing pressure on land use (Gencer, 2013; Scherer and Endlicher, 2014). As cities are hubs of hubs of economic, political and cultural activity, and centres of knowledge and innovation (UN Habitat, 2014) negative impacts on their infrastructure constitute a serious thread (Carter et al., 2015; Solecki et al., 2015). As one consequence of alleviated air temperatures, energy demand for cooling is going to increase (Uejio et al., 2011). Power blackouts and infrastructure failures could be further consequences (Allegrini et al., 2015; Gosling et al., 2009; Loughnan et al., 2013).

Risk assessments help to identify vulnerable population and infrastructure, such providing valuable information for governments and planners where to direct resources for adaptation and mitigation efforts (Wilhelmi et al., 2004). Heat risk is captured as being a product of hazard and vulnerability (Dugord et al., 2014; Nadim, 2013). Vulnerability, commonly defined as a function of exposure, sensitivity and adaptive capacity (Loughnan et al., 2013; Solomon et al., 2007), varies between geographic locations and populations groups (e.g. Chuang, 2013; Krüger et al., 2013). Even intra-urban variety within one city can be high (Schuster et al., 2014), such, vulnerability towards heat stress is highly dependent on the local context (Benzie, 2012). Strong neighbourhood ties are reported to decrease the likeability to suffer from high temperatures (Harlan et al., 2006). Other influencing factors are for example the quality of housing and the built environment, the local urban geography, lifestyle, health status, income, employment, tenure, social networks and self-perception of risk (e.g. Bao et al., 2015; Carter et al., 2015; Loughnan et al., 2013; Scherer et al., 2014).

Though mapping of vulnerability to heat stress helps to identify geographic 'hot spots' and to direct prevention efforts (Wilhelmi et al., 2004), it only begins to be part of risk assessment agendas (Wolf et al., 2011). Many studies either focus on modeling of heat impacts only, but don't consider the inhabitant's sensitivity towards heat stress (Allen et al., 2011; Chatzipoulka et al., 2015; Lindberg et al., 2016; Musy et al., 2015), or concentrate on developing vulnerability indexes without assessing the spatially explicit heat hazard (Benzie, 2012; Buchin et al., 2016; Oudin Åström et al., 2015). Often heat stress is derived from punctual air temperature measurements (Dugord et al., 2014, Loughnan et al., 2013) or from remote sensing products (Uejio et al., 2011; Wolf et al., 2011). While the latter is more spatially explicit, it provides solely information about surface temperature and neglects other influencing factors on thermal comfort, such as radiation and wind. Contrary, mean radiant temperature (T_{mrt}) is found to be a representative indicator of thermal comfort conditions in the external environment (Musy et al., 2006; Jänicke et al.; 2015, Chatzipoulka et al., 2015; Thorsson et al., 2007). It represents the sum of all shortwave and longwave radiation fluxes to which the human body is exposed (Lindberg and Grimmond, 2011) and is either assessed by measuring or modeling.

Furthermore, most heat risk assessments focus on nation or city level (Romero-Lankao et al., 2012), while only few are concerned with the neighbourhood-level (e.g. Uejio et al., 2011; Johnson et al., 2012). However, investigations on neighbourhood-level bear the potential for more specific risk information as they can be adapted to the local context and thus provide more concrete evidence for planners (Wilhelmi et al., 2004; Norton et al., 2015). Risk mitigation measures aim to reduce the risk to tolerable or acceptable levels (Nadim, 2013). Heath health warning systems, promotion of tree plantings and public education constitute exemplary measures. However, their effectiveness is largely dependent on the local context, which is why they should be based on place specific risk assessments. Low spatial resolution of census data often prevents investigations on even finer scales (Wolf et al., 2011). Regarding this conflict between geographical specificity and data privacy issues, Schuster and colleagues (2014) see the neighbourhood scale as the best compromise.

The approach presented here is based on neighbor-hood level and employs T_{mrt} as an indicator to assess thermal comfort conditions. For continuous spatial information, T_{mrt} is modelled with the solar flux model SOLWEIG (Lindberg and Grimmond, 2011), allowing to detect spatial variability. Socio-economic data and physical environment indicators are used to develop a vulnerability index for extreme heat. Combining the hazard layer and vulnerability layer, the heat risk is determined and high risk areas are identified. The role of vegetation and site characteristics are explored since these are known to play an important role in heat mitigation. The case study area Maxvorstadt represents an inner city district of Bavaria's capital city Munich. On city scale, an urban climate analysis was performed in 2014 to assess the current thermal conditions (source!!). However, due to the big scope, modelling resolution was restricted to 50x50m, considering only building blocks. The work presented here combines fine scaled (2x2m) thermal modelling data with vulnerability information. In doing so, the following research questions will be answered:

- Where are the areas in Maxvorstadt with the highest T_{mrt} during a heat day?
- What is the influence vegetation coverage and urban geometry on T_{mrt}?
- Which indicators should be considered to assess the heat risk at neighbourhood-level?
- Which parts of Maxvorstadt bear the highest heat risk?
- (*Which measures can be taken to improve the situation of the most affected areas*?)

The subsequent section explores the theoretical background on heat stress, vulnerability assessment and mitigation by green infrastructure. Section 3 introduces the study area, provides an overview of the methodical approach and explains the analytical steps. Assessment results are presented in Section 4 and discussed in Section 5. Section 6 summarizes the main findings of this study and outlines objectives for further research.

2 Theoretical background

2.1 Heat stress assessment and heat stress in cities

2.1.1 Heat health impacts on humans and heat thresholds

Research on heat stress and human health has expanded rapidly since the early 1990s in various academic disciplines (Gosling et al., 2009; Wilhelmi and Hayden, 2010). Heat cramps, heat exhaustion, heat rash, heat stroke, all associated with the inability to balance the heat flows from the human body by the thermoregulation system, have been identified as direct heat impacts on human health (Buchin et al., 2016; Smoyer-Tomic et al., 2003). Indirect effects relate to increased risk of death from pre-existing cardiovascular and respiratory diseases (Smoyer-Tomic et al., 2003, Hallegatte et al., 2011) and degraded air quality as the concentration of pollutants increases (ten Brink et al., 2006). Meteorological variables influencing human illnesses and deaths during heath waves include relative humidity, wind speed, fluxes in short- and long-wave radiation and temperature (Wilhelmi et al., 2004).

Analysing mortality data represents a common approach to detect temperature-health interactions. Heat-related death are usually estimated by subtracting the expected mortality (also called baseline mortality) from the observed mortality (Gosling et al., 2009). However, reviewing heat-mortality relationship studies, Gosling et al. (2009) report low comparability of outcomes since methods to define baseline mortality and heat stress events differ. Similarly, Buchin et al. (2016) affiliate disagreements in heat-related mortality data to the methods to define days or episodes of heat stress, the use of different types of mortality data, methods to account for displaced deaths, or the methods to estimate base mortality rates.

While a common approach to define base mortality rates could be more easily agreed upon, perceptions of heat days are largely dependent on the local climate (Harlan et al., 2006). Even though heatwaves are meteorological events, they are more usually defined with reference to human health impacts (Robinson, 2001; Xu et al., 2016). Such, there is no international threshold temperature for classification as a "hot day" or international definition of heatwave (Gosling et al., 2009; Xu et al., 2016). For example in Australia and the US no single universal threshold temperature exits since tolerance of excess heat is seen to vary regionally according to the population and its preparation for hot weather (Gosling et al., 2009; Loughnan et al., 2013). Generally, thresholds tend to be higher for locations with relatively warmer climate (Donaldson et al., 2003). As regards Germany, the German Meteorological Service (DWD) characterizes days with a maximum air temperature above 25°C as summer days and above 30°C as heat days. Nights with minimum air temperatures never falling below 20°C are labelled tropical nights (DWD, 2016a). For comparison, corresponding thresholds for North East England are 28°C

(day) and 15°C at night (Gosling et al., 2009), while Lisbon has a daytime threshold of 32°C (Oliveira et al., 2011).

Heatwaves are often described using a combination of intensity and duration (Gosling et al., 2009; Xu et al., 2016). In their heat impact study for North-Rhine-Westphalia, Lissner et al. (2012) delineate periods of minimum three consecutive days with Tmax greater 30°C as heat-waves. Studying Greater Manhattan, Kovats (2004) regards periods of six or more days above 30°C as heatwaves. Other authors use relative rather than absolute thresholds: Gosling et al. (2007) specify three or more days above the 95th temperature percentile as heatwaves, while Hajat et al. (2002) relate to five consecutive days greater than the 97th percentile. Comparing 60 heat wave definitions, Xu et al. (2016) conclude that the duration of extreme heat exposure which significantly increases mortality risk varies across different regions, yet most authors choose two to four days for their definition without specifically reasoning why. Maximum, mini-mum, mean air temperatures or apparent temperature as well as heat index are employed as temperature indicators, with no one being superior so far (Xu et al., 2016). In fact, optimal indi-cators may vary across different cities and age groups, such vulnerable groups should be given the most attention (Xu et al., 2016).

The German Meteorological Service (DWD) has developed a graded warning system for heat days particularly addressing inhabitants of residential homes and the elderly population (DWD, 2016b). Warning level 1 is reached if the perceived temperature in the early afternoon exceeds 32°C for at least two consecutive days. Warning level two is issued if the perceived temperate exceeds 38°C (DWD, 2016b). Though the longest heat waves are the deadliest (Gosling et al., 2009; Hajat et al., 2002), intensity seems to be more important than duration regarding health impacts (Xu et al., 2016). High overnight temperatures have an especially hazardous effect as there is no relief from the daily heat (Loughnan et al., 2013). Interestingly, higher excess mor-tality rates are related to heat waves striking early in the warm season than to later ones (Hajat et al., 2002; Smoyer et al., 2003) and the year's first heat wave has greater impact than the second one (Hajat et al., 2002; Páldy et al., 2005), pointing towards an acclimatization effect. In areas with common hot and humid summer conditions physiological, behavioral and infrastruc-ture adaptation is more likely, leading to reduced negative impacts (Smoyer-Tomic et al., 2003).

2.1.2 Thermal comfort indices

As already depicted above, different bioclimate indices are used to assess human heat stress: air temperature (Dugord et al., 2014; Loughnan et al., 2013), land surface temperature (Carter et al., 2015; Uejio et al., 2011; Wolf et al., 2011), mean radiant temperature (Chatzipoulka et al., 2015; Jänicke et al., 2015; Lindberg et al., 2016; Musy et al., 2015) and apparent temperature (Kershaw and Millward, 2012). Blazejczyk et al., (2012) report that over 40 indices were or are in use throughout the world to define thermal comfort.

Of the indices based on direct measurements of environmental variables, air temperature (T_{air}) is reported as being less reliable, since other important factors for the human body energy balance, such as humidity, radiation, wind and precipitation are neglected (Gill et al., 2007). Land-surface temperatures can be easily obtained via remote sensing and satellite imagery, but are seen as less useful for assessing human heat stress due to low temporal resolution (Wilhelmi et al., 2004) and potentially erroneous information when dealing with complex three-dimensional structures as is the case in heavily built-up locations (Kershaw and Millward, 2012). Physiological equivalent temperature (PET) belongs to the group of indices based on the human energy balance (Blazejczyk et al., 2012; Matzarakis et al., 2015) and takes into account meteorological parameters (T_{air}, air humidity, wind speed and T_{mrt}) as well as thermo-physiological elements (clothing, activity and age) (Mayer, 1993). Like Universal Thermal Climate Index (UTCI) (Jendritzky et al., 2012) it represents a sophisticated index for assessing human thermal comfort, yet several authors suggest that T_{mrt} alone constitutes a good predictor for heat stress and heat mortality (Mayer, 1993; Thorsson et al., 2014). On clear and calm days, T_{mrt} is reported to be the most important meteorological parameter influencing human energy balance and heat load (Gill et al., 2007; Lindberg et al., 2016; Oliveira et al., 2011) as it has the largest influence on PET (Ketterer and Matzarakis, 2014; Matzarakis et al., 2010). T_{mrt} represents "*the net result of all shortwave- and longwave radiation fluxes (both direct and reflected) from the surroundings to which the human body is exposed*" (Lindberg and Grimmond, 2011, p. 623).

Three different approaches for estimating T_{mrt} exist: The most accurate method is to use pyranometers and pyrgeometers, arranged in six directions, namely upward, downward and from the four cardinal points, to measure the short-wave and long-wave radiation fluxes (Lindberg et al., 2014). A less costly and time-consuming approach is represented by the globe thermometer, which has originally been developed for indoor measurements. However, it has hardly been validated in outdoor environments (Thorsson et al., 2007). As a third approach, several computational models have been developed for the calculation of T_{mrt} from short and longwave radiation fluxes: Rayman (Matzarakis 2007), ENVI-met and SOLWEIG (Lindberg et al., 2008) constitute well established examples (Jänicke et al., 2015; Onomura et al., 2015). These models assess T_{mrt} less accurate compared to direct measurements with the first approach (Thorsson et al., 2007), but have no acquisition costs since the software is freely available for research purposes and offer the possibility to evaluate influences of single parameters and alternative planning scenarios.

2.2 Vulnerability towards heat stress

2.2.1 Vulnerability concept and influencing factors

Generally, vulnerability is defined as the 'propensity or predisposition to be adversely affected' (IPCC 2012, p.5). In the context of climate change, vulnerability is described as "a function of exposure to climate impacts, sensitivity to those impacts and the adaptive capacity of the people or systems impacted" (IPCC, 2007, p. 883). Or, as regards disaster risk management, seen as being directly related "to the susceptibility, sensitivity and lack of resilience or capacities to cope with and adapt to extremes and non-extremes" (IPCC, 2012, p.70). In both cases, vulnerability is determined by a combination of environmental, economic and social factors (Loughnan et al., 2013). Risk is often perceived as a combination of the hazard's magnitude and the vulnerability of exposed population and infrastructure (IPCC, 2012). However, concepts of vulnerability, risk and their contributing elements differ between various schools of thought and scientific disciplines (Chuang, 2013; Depietri et al., 2013; Dugord et al., 2014). For example, Depietri et al. (2013) rather consider vulnerability as the result of exposure, susceptibility and lack of resilience. Adapative capacity is seen as part of a superior risk framework (Depietri et al., 2013). According to Dugord et al. (2014), exposure refers to the number and location of the population exposed to the impact, while for (Wilhelmi and Hayden, 2010) exposure relates to the hazard itself and is most commonly estimated by quantitative environmental modeled or measured data. Both sensitivity and adaptive capacity link with the physiological and socio-economic condition of the exposed population and infrastructure (Dugord et al., 2014), often expressed in quantitative demographic data (Wilhelmi and Hayden, 2010). This analysis follows the IPCC definition and sees vulnerability as a compound of the three elements exposure, adaptive capacity and sensitivity (see figure 1).
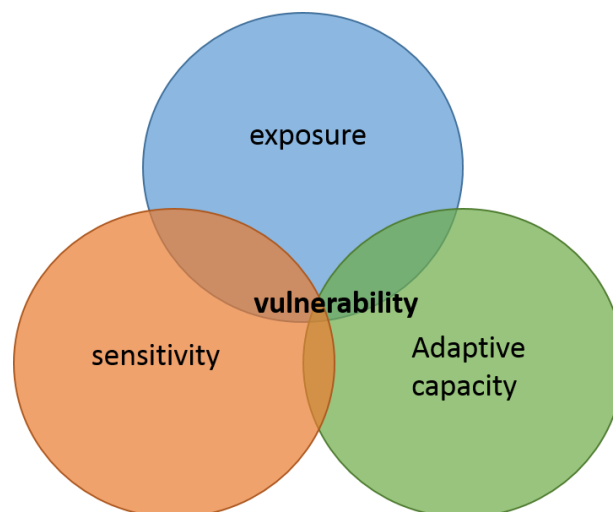
Figure 1: Vulnerability concept (own figure)
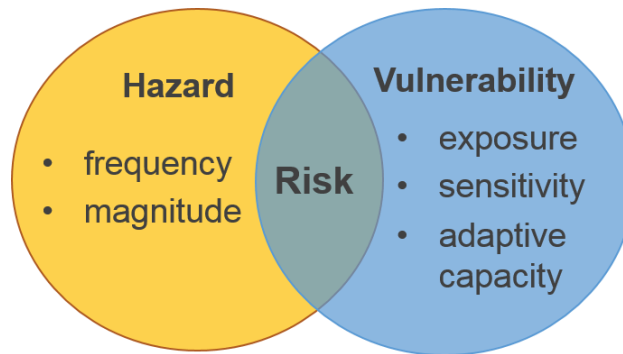
Vulnerability is highly dependent on context, as importance of influencing variables varies across space and time (Bao et al., 2015; Romero-Lankao et al., 2012). In a comparison of heat wave vulnerability in Philadelphia and Phoenix, Uejio et al. (2011) reported that major determinants for the latter were night-time temperatures and housing density, whereas for Philadelphia, minority status and the year the house was built were decisive. Chow et al. (2012) however observed significant changes in vulnerability patterns of Phoenix between 1990 and 2000, underlining that vulnerability is not a static, but dynamic concept. Moreover, it is suggested that vulnerability varies not only between geographic locations and time, but also within social groups (Benzie, 2012). Age has been identified as one decisive factor for being negatively affected by heat (Johnson et al., 2012; Loughnan et al., 2013; Reid et al., 2009; Wolf and McGregor, 2013): Older people (commonly defined as older than 65 years) constitute the majority of heat wave victims not only in Europe, but also worldwide (Brown and Walker, 2008). This is affiliated with a limited capability of the human body to respond to alleviated temperatures and the higher probability of having pre-existing cardiovascular and pulmonary illnesses among the elderly (Bao et al., 2015; Brown and Walker, 2008). Besides, the very young population (younger than three years) show a high sensitivity towards heat, since their physiological capabilities are also reduced (Bao et al., 2015; Loughnan et al., 2013). Pre-exisiting medical conditions (physically or mentally) (Carter et al., 2015; Tomlinson et al., 2011), low education level (Reid et al., 2009; Wolf et al., 2011) and social isolation (Benzie, 2012; Loughnan et al., 2013) are further widely reported risk factors. It is argued that people living on their own tend to ignore or miscalculate the heat risk and are more likely to lack support in case of emergency (Bao et al., 2015; Depietri et al., 2013). Similarly, inability to speak the official language and minority status are associated with higher risk from heat (Carter et al., 2015; Harlan et al., 2006). This is explained by the observation that minority groups tend to cluster in deprived neighbourhoods with high exposure to heat and lack of public support and cooling amenities (Chow et al., 2012).

Such, not only personal characteristics and self-perception of risk, but also living arrangements (Carter et al., 2015) and the quality of housing and the local environment (Benzie, 2012; Brown and Walker, 2008) play an important role. Low quality housing (Wolf et al., 2011) and living on the top floor of a flat or high-rise building (Brown, 2011; Tomlinson et al., 2011) increase the likeability to suffer from high temperatures. Having access to green space or living in a densely

vegetated neighbourhood raises the resilience towards high temperatures since vegetation provides cooling through shading and evapotranspiration (Bao et al., 2015; Harlan et al., 2006). Strong social networks provide support in critical situations and can play a major role for reducing heat vulnerability (Bao et al., 2015; Romero-Lankao et al., 2012): Chuang (2013) noted that wealthy neighbourhoods in Phoenix with less social stability and higher neighbourhood mobility were more vulnerable to heat stress than disadvantaged, but socially cohesive neighbourhoods.

2.2.2 Heat vulnerability index

Building indicator frameworks and aggregating them into a heat vulnerability index (HVI) represents a common approach in urban vulnerability assessments (Romero-Lankao et al., 2012). According to Wolf et al. (2011), a vulnerability index should be significant, robust, relevant, feasible and transferable. However, due to the context dependency of vulnerability and different concerns of different disciplines, no international HVI exists, instead several case-study specific HVI have been developed (Chuang, 2013; Chuang and Gober, 2015).

In their review of heat vulnerability assessments, Bao et al. (2015) present an overview of 15 HVI, providing information about study location, used indicators and chosen method for building the HVI (see appendix). While the number of indicators used ranges from just 5 (Tomlinson et al., 2011) to as much as 25 (Hondula et al., 2012), hazard magnitude constitutes the only factor that has been extensively studied. Aggregation approaches are equally diverse: Some researchers assumed the indicators to be of equal importance and weighted them equally, others employed expert judgement or multivariate statistical techniques (e.g. principal component analysis) to assign individual weights (Bao et al., 2015). The authors suggest that selection and weighting of indicators should refer to local characteristics, while heat-related health outcomes can be used as a start (Bao et al., 2015).

Reviewing 54 studies, Romero-Lankao et al. (2012) found that mostly 13 factors have been used as proxies for heat vulnerability: hazard magnitude (i.e., temperature level), population density, age, gender, pre-existing medical conditions, education, income, poverty, minority status, acclimatization, and access to home amenities (such as air conditioning). Contrary to high agreement on the role of pre-existing medical conditions and age, dissension exists regarding the influence of income, housing density and social networks on heat vulnerability as some studies reported indifference or even reverse impacts (Romero-Lankao et al., 2012).

In order to increase comparability between study results, Reid et al. (2009) designed a nationwide HVI for the United States, considering 10 variables: poverty, education, ethnicity, living alone, population older than 65 years, aged people living alone, vegetation, diabetes, lack of central air conditioning (AC), lack of any AC. Though several studies (e.g. Mayer et al., 2014; Bradford et al., 2015) adapted the approach of Reid and colleagues, their index has been shown to misjudge health outcomes in some states due to local influences (Chuang, 2013; Reid et al.,

2012). As regards Germany, Krüger et al. (2014) developed a settlement heat sensitivity index (SHSI), based on city structure types, demographic (population density, age cohorts) and thermal data (PET-values at 2pm calculated from air temperature). The SHSI is gained by multiplying the PET factor with the mean of the factors city structure type and demographic situation and is expressed on a scale from low to high level of concern (Krüger et al., 2014). City structure types are roughly classified in four groups according to their warming potential, thus there is no detailed consideration of differences between e.g. block or chain buildings. Krüger et al. (2014) note that SHSI's applicability would be increased if information about distance between sensitive areas and thermal comfort zones such as parks and about spatial distribution of sensitive infrastructure, e.g. hospitals, retirement homes and nurseries, would be considered. Influencing, though relatively unexplored are factors like extent and quality of housing as well as availability of supporting infrastructure (e.g. hospitals, information center) and public aid (Carter et al., 2015).

It is often observed that vulnerable population groups concentrate in those areas where heat loads are highest (Lindley et al., 2011). Carter et al. (2015) found this form of environmental injustice in their study of Greater Manhattan, where deprivated neighbourhoods showed the highest UHI values. However, as it is acknowledged that vulnerability is often linked to deficits in risk communication, leading to wrong risk perceptions and inappropriate behavior (IPCC, 2012), explicit consideration of social justice issues is likely to improve outcomes of adaptation measures for vulnerable people (Benzie, 2012). Spatially explicit risk or vulnerability assessment can provide valuable information in this regard.

2.3   Response strategies towards heat risk and the role of green infrastructure

Generally, climate change response strategies either try to reduce the hazard to acceptable or tolerable levels (mitigation) or to reduce the vulnerability and exposure of the population, infrastructure and other elements at risk (adaptation) (Carter et al., 2015; Fryd, 2011; Nadim, 2013).

Main approaches to increase the resilience of humans and natural systems include adaptation in buildings and housing, e.g. by air conditioning and building design (Gabriel and Endlicher, 2011; Uejio et al., 2011), educational activities about protection of individuals from heat impacts (Wolf et al., 2011) and heat health warning systems (Loughnan et al., 2013; Wilhelmi and Hayden, 2010). As already mentioned in section 2.1.1, the German Meteorological Service (DWD) has developed a graded warning system for heat days particularly addressing inhabitants of residential homes and the elderly population (DWD, 2016b). Literature findings suggest that the success of these warning systems is depending on the availability of effective intervention strategies (Kalkstein et al., 2009; Wolf et al., 2011), which can be buddy systems among neighbours,

hotline telephone service providing advice on appropriate behavior (Wolf et al., 2011) or designation of "cooling centers" such as museums and libraries that provide refuge from the heat for pedestrians (Bradford et al., 2015). For several reasons, air conditioning is seen as mal-adaptation: Firstly, air conditioning systems demand additional energy usage and are such likely to increase the production of greenhouse gas emissions (xx). Furthermore, their waste heat contributes to UHI and may increase heat exposure for the external environment (Uejio et al., 2011). Finally, inequity between the economically advantaged and disadvantaged may expand, if only the former are able to afford installation of a cooling system (Gosling et al., 2009).

Heat mitigation techniques aim to improve the thermal budget of cities by increasing thermal losses and decreasing the corresponding gains. Since urban form, surface material/pavements and green spaces are considered to have a major influence on urban temperatures (Gago et al., 2013), prominent approaches in this regard focus on increasing the urban environment's albedo with reflexive surfaces, on expanding green spaces and on making use of natural heat sinks to dissipate excess heat (Santamouris et al., 2014).

Prevalence of open spaces or densely built up areas has influence on heat storage and wind porosity of the city (Wang and Akbari, 2016). Skyviewfactor (SVF) and groundviewfactor (GVF) are two measures for the openness of the sky and the sun, respectively. While SVF is constant, GVF varies in time as it is depending on the sun's position (Chatzipoulka et al., 2015). It provides information if a certain spot at a certain time is sunlit or not. Both measures are influenced by building height, street width and the corresponding height to width ratio (see figure 2), whereas the street canyon's orientation is also decisive for GVF (Norton et al., 2015).
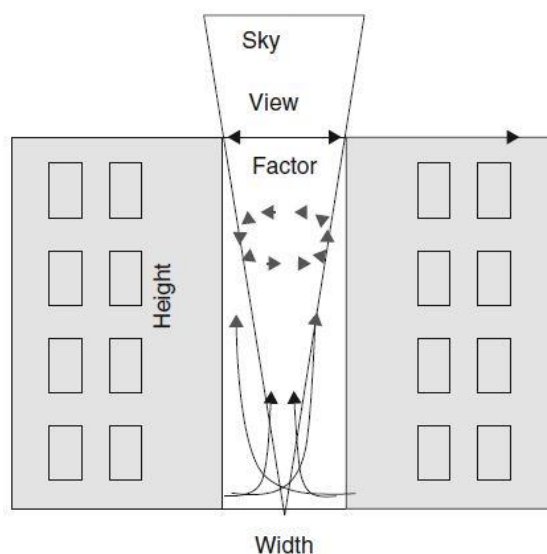
Figure 2: Sky view factor and influencing parameters (Source: Raven 2010, p. 457)

Notably, effects of different urban forms on temperature vary over time: Open spaces obtain more solar radiation during daytime, but release more heat during nighttime than urban canyons as emission of shortwave radiation is not hampered (Wang and Akbari, 2016). Similarly, streets with a low H/W ratio experience higher heat stress during daytime, but also better nocturnal cooling compared to streets with high aspect ratio (Herrmann and Matzarakis, 2012). Narrow self-shading street canyons provide benefits for pedestrians under summer conditions, while limiting solar access in winter (Ali-Toudert and Mayer, 2006; Ketterer and Matzarakis, 2014). North-south oriented streets feature lower Tmrt than east-west oriented streets (Ketterer and Matzarakis, 2014; Kuttler, 2011). Street canyons with an orientation of 75-90°C show the highest frequency of heat stress throughout the year (Ketterer and Matzarakis, 2014). Ketterer and Matzarakis (2014) found that for southern Germany, northwest-southeast oriented street canyons with an H/W of 1.5 seem to be the best choice for urban street design.

Urban green space is important for lowering temperatures, as it cools through evapotranspiration, stores and reradiates less heat than built surfaces, provides shading and guides wind directions (Gago et al., 2013; Gill et al., 2007; McPherson et al., 1994). Investigating different settlement types and surface fractions, Buchholz and Kossmann (2015) concluded that a minimum surface fraction of 20% should be reserved for vegetation. Settlements types with more than 50% of their area occupied by buildings, should increase their vegetation fraction up to 30% to maintain tolerable outdoor heat conditions (Buchholz and Kossmann, 2015). Evaluating countermeasures to urban heat island, Buchin and colleagues (2016) found that trees performed best in attenuation or reflection of short-wave radiation. Regarding indoor temperatures, the authors favored passive cooling (through night ventilation, shading elements) and evaporative cooling (through green facades) (Buchin et al., 2016). The literature suggests several benefits of mitigation by urban green infrastructure: While modification of urban morphology is mostly only possible in new developments and demands long-term urban planning, urban green can be fitted to existing urban form (Norton et al., 2015). Moreover, it has the potential to reduce temperatures without increasing energy use and greenhouse gas immissions (Doick et al., 2013), and provides additional benefits such as carbon sequestration, air pollution removal, rainfall interception and provision of recreational space (McPherson et al., 2016; Meier and Scherer, 2012; Norton et al., 2015).

Green infrastructure options for cooling can be differentiated in four categories: green roofs, vertical greening, green spaces, street trees (Gago et al., 2013; Norton et al., 2015). Green roofs are found to decrease urban surface temperatures and reduce cooling demand of buildings (Norton et al., 2015). Though modelling suggests that green roofs can cool at neighbourhood-scale if covering a large area (Gill et al., 2007), the main effect is restricted to the buildings where they are installed, providing little cooling relief on street level (Musy et al., 2015). Green facades can be beneficial for pedestrians when they are installed adjacent to walkways (Norton

et al., 2015) and have the greatest effect on dark walls and on those with a high solar exposure (Wong et al., 2010).

The cooling potential of urban green space is largely influenced by size, type and composition of vegetation (Doick et al., 2013; Feyisa et al., 2014). The highest cooling effects in settlement areas are observed for heterogeneous vegetation structures, featuring grassland, bushes as well as small and high trees (Lehmann et al., 2014). Large urban parks are not only reported to create cool islands (Shashua-Bar and Hoffman, 2000), but also to have an cooling impact on the surrounding built areas (Doick et al., 2013; Norton et al., 2015; Oke, 1988). The cooling influence of large Chapultepec Park (500 ha) in Mexico City was assessed to reach a distance of about 2 km of the park with an temperature difference of 4°C between the park and built up areas (Jauregui, 1990). In order to achieve cooling at significant distances beyond the site boundaries, Doick et al. suggest that greenspaces and wider green infrastructure should be a minimum of 0.5 ha. However, depending on type and density of vegetation, also small parks feature significant temperature differences: Oliveira et al. (2011) found a park cool island of 4.8°C for park of 0.24 ha size in Lisbon. A network of many small, well distributed urban green spaces is supposed to yield a collective net cooling impact on city scale (Yu and Hien, 2006), while benefitting a larger number of neighbourhoods (Norton et al., 2015).

Street trees provide cooling through evapotranspiration and shading, reducing heat stress for pedestrians and cooling demand for buildings (Coutts et al., 2014; Bowler et al., 2010). Using the i-Tree model, McPherson et al., (2016) assessed that the 9,1 million street trees in California yielded annual electricity savings of 684GWh or 74.9 kWH per tree. The total annual value of street tree services was as much as $1.0 billion, or $110.63 per tree (McPherson et al., 2016). Trees over asphalt have more direct cooling effect to the area than trees over grass, while deciduous and broadleaf trees have a higher cooling capacity than coniferous trees (Meier and Scherer, 2012). To avoid heat trapping under dense tree canopies at night and reduction of wind flow (Sinnett et al., 2015), it is suggested that street trees should not form a continuous canopy (Spronken-Smith and Oke, 1999). Furthermore, water and tree growth demands, maintaining costs, light penetration in winter and selection of diverse and climate resilient species have to be considered (Doick et al., 2013; McPherson et al., 2016). Thus, effectiveness and benefits of green infrastructure mitigation strategies depend largely on the location and respective site characteristics. Norton et al. (2015) summarize cooling characteristics of UGI mitigation strategies and define priority locations (see table x). While trees should be planted in wide streets and green open spaces, vertical greenery constitutes an option for narrow street canyons. Low, large as well as poor insulated buildings are favourable locations for green roofs.

Table 1: modes of cooling provided by different urban green infrastructure options and priority locations (Source: Norton et al., 2015, p.132)

UGI	Green open spaces	Trees	Green roofs	Vertical greening
Shades canyon surfaces?	Yes, if grass rather than concrete	Yes	Shades roof, not internal canyon surfaces	Yes
Shades people?	Yes, if treed	Yes	No, only very intensive green roofs	No
Increases solar reflectivity?	Yes, when grassed	Yes	Yes, if plants healthy	Yes
Evapo-transpirative cooling?	Yes, with water	Yes (unless severe drought)	Yes, with water when hot	Yes, with water when hot
	No, without water		No, without water	No, without water
Priority locations	Wide streets with low buildings – both sides Wide streets with tall buildings – sunny side	Wide streets with low buildings – both sides Wide streets with tall buildings – sunny side In green open spaces	Sun exposed roofs Poor insulated buildings Low, large buildings Dense areas with little available ground space	Canyon walls with direct sunlight Narrow or wide canyons where trees are unviable

3 Methodology

3.1 Study area Maxvorstadt

The study area is located in Munich, Bavaria's capital city in the South of Germany. With more than 1,5 million inhabitants, Munich represents the third largest city in Germany and has continuously increasing population numbers (Portal München, 2016a). Situated 520 m a.s.l. in Middle Europe, Munich's climate can be characterized as warm temperate with a mean temperature of 9,1°C, and a yearly precipitation of 959 mm (LH München, 2014). During summer month (June to August), the city's wind flows are influenced by a local wind circulation system called alpine pumping. Under cloud-free conditions, warm air is transported to the Alps as they heat up quicker, while during nighttime cool air flows back from the Alps (Mayer and Matzarakis, 1992). According to the Urban Climate Analysis Munich, the city of Munich is going to experience an increase of heat days (daily maximum temperature > 30°C) from currently 8 to over 44 heat days by 2100 (LH München, 2014). Maxvorstadt, home of 52.575 inhabitants (3,5% of Munich's population), is located close to Munich's city center (Portal München, 2016b, see figure 3).
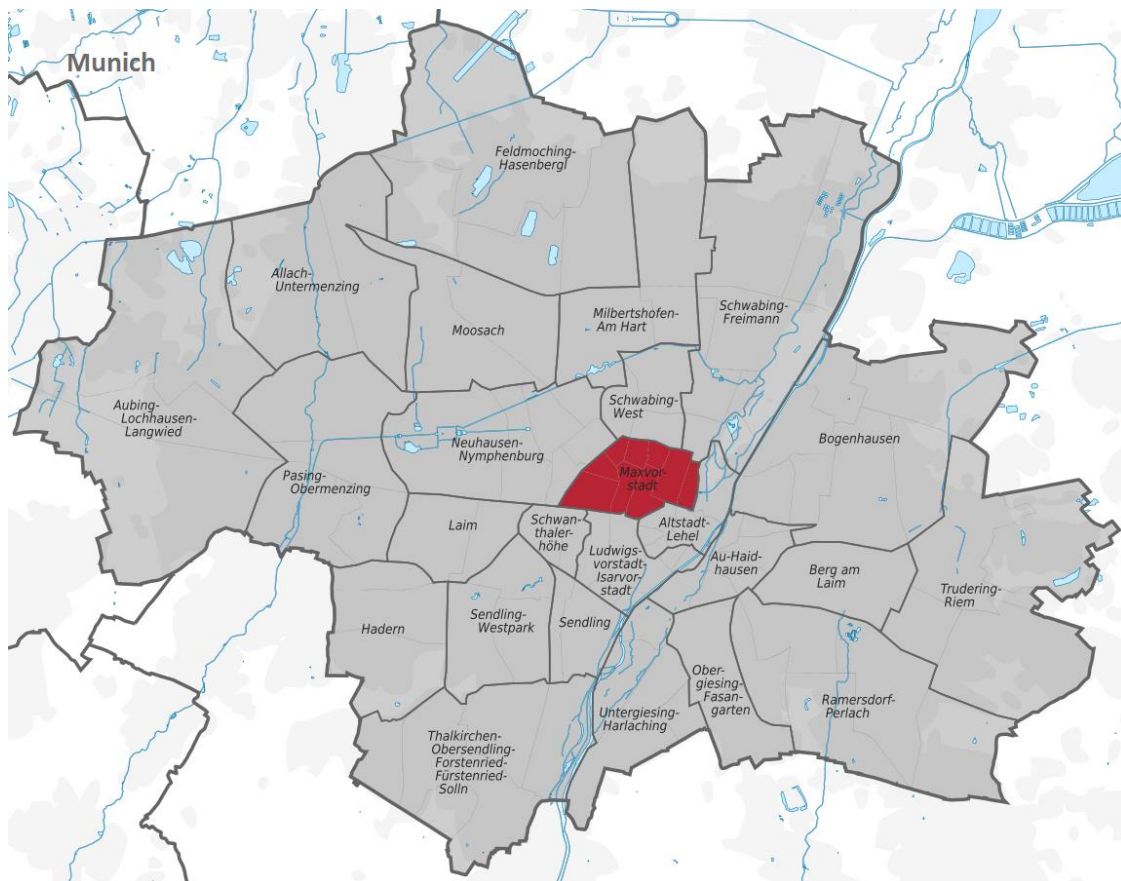
Figure 3: Munich and location of city district Maxvorstadt (TUBS, CC BY-SA 2.0, www.wikipedia.org/Maxvorstadt)

Maxvorstadt is one of the most busiest city districts of Munich: During the day, up to four times more people than actually live in the area spend their time there (Portal München, 2016b). The

city district hosts Munich's two universities, several universities of applied sciences and is known as a centre for art due to its large number of museums (Portal München, 2016b). Its population mean age lies between 20 and 30 years, and the numbers of older people and little children are relatively small compared to other city districts (see appendix 2). Nevertheless, the city district has the fourth highest population density of Munich (122 EW/ha) and the highest percentage of one-person households (68.4%, Munich: 54.4%) (Statistisches Amt, 2015). Maxvorstadt consists of nine city district parts (see figure 4) and its building structure is mainly dominated by perimeter buildings. City district part characteristics will be explored in section 4. In the urban climate analysis Munich, Maxvorstadt was attested an unfavourable bioclimatic situation with little nocturnal cooling (LH München, 2014). Due to the analysis' rough resolution of 50 x 50m, specific information is missing.
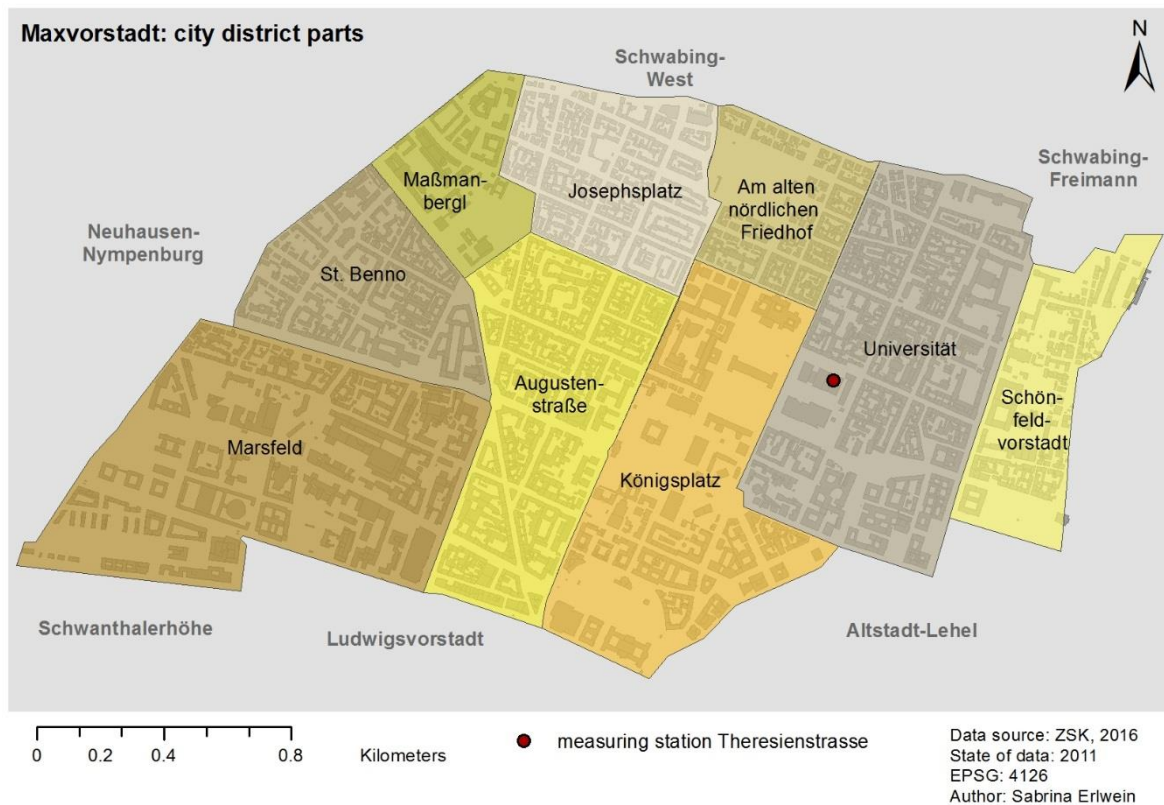
Figure 4: Map of Maxvorstadt's city district parts and location of measuring station (own figure)

3.2 Methodological approach

The risk analysis follows a three-stepped approach (see figure 5): First, the heat stress is estimated by modelling T_{mrt} distribution for one heat day using the solar flux model SOLWEIG. Second, vulnerability is assessed for each city district part with the help of socioeconomic and environmental indicators. In a third step, high risk areas are identified by combing hazard and vulnerability information. Furthermore, insights from former modeling steps are used to suggest mitigation measures.
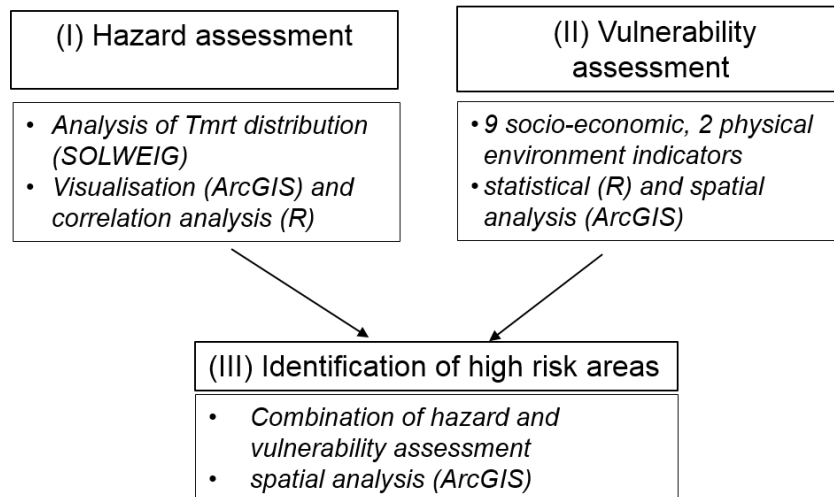
Figure 5: Three stepped risk assessment approach

3.2.1 Hazard assessment

The T_{mrt} distribution is assessed using the freely accessible solar flux model SOLWEIG (Solar and long wave environmental irradiance geometry model). SOLWEIG was developed by Lindberg et al. 2008 and requires high resolution digital elevation models (DEM) of buildings and vegetation, up to minutely data of relative air humidity, ambient air temperature and solar radiation as an input (Lindberg et al., 2016a). This data given, first skyview (SVF) and groundviewfactors (GVF), then incoming (-down) and outgoing (-up) shortwave (k-) and longwave (l-) radiation fluxes are calculated (see figure 6) (Lindberg and Grimmond, 2011). R represents the sum of all fields of long and shortwave radiation in three dimensions, from which T_{mrt} is calculated using Stefan-Boltzmann's law (Lindberg and Grimmond, 2011). For detailed equations see Lindberg et al. 2016a, pp. 2-4.

As recommended by Lindberg and Grimmond, albedo of ground and walls was left to 0.2, emissivity of walls to 0.9 and of ground to 0.95. Transmissivity of vegetation was set to 0.02. Default values were also used for personal parameters: a factor of 0.7 for absorption of shortwaves and 0.95 for absorption of longwaves respectively.
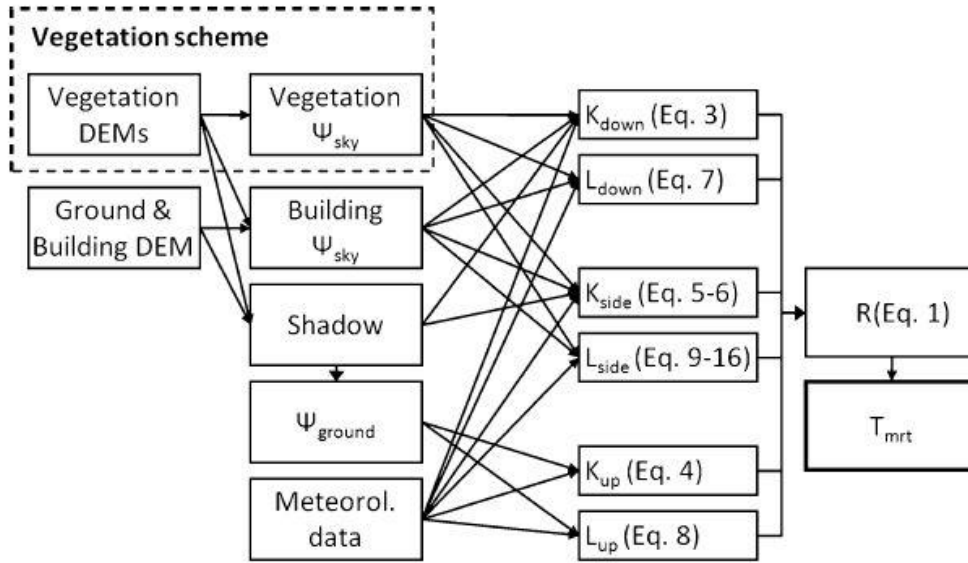
Figure 6: Workflow chart for SOLWEIG (Source: Lindberg & Grimmond 2011, p.3)

Table 1: Variables used as in input in SOLWEIG 2015a

Name	description	Unit
k_{down}	incoming shortwave radiation	W/m²
l_{down}	incoming longwave radiation	W/m²
k_{side}	shortwave radation from four cardinal points	W/m²
l_{side}	longwave radiation from the four cardinal points	W/m²
k_{up}	outgoing shortwave radiation	W/m²
l_{up}	outgoing longwave radiation	W/m²
R	mean radiant flux density	W/m²
Ψ_{ground}	ground view factor	-

A DEM of Maxvorstadt (year 2011, resolution 0,2m x 0,2m) was provided by Geodatenservice Munich, which was separated into a building and vegetation DEM with the help of a vegetation mask (year 2011) granted by the Centre for Urban Ecology and Climate Adaptation. Both DEMs were transformed to ASCII-format to fit for SOLWEIG. Hourly meteorological data from the weather station "Theresienstraße" were obtained from the Meteorological Institute Munich (MIM), operated by the physical department of the Ludwigs-Maximilians University. The weather station's location in the research area (see figure 4) constitutes a major advantage compared to other studies using weather data from stations placed outside the city with quite different climatic conditions than in the city core. Time series of measurements 2m above the ground (years 2000-2006) as well as records for all heat days (Tmax > 30°C) from 1982 to 2016 (see appendix 3) offered by the MIM were analysed to find a time period with severe heat stress. In July 2006, Maxvorstadt experienced 18 heat days, making it the month with the highest number of heat

days recorded (MIM 2016). For selecting the modelling day, the following criteria were set: In order to find the most vulnerable places under heat stress conditions, daily T_{air} max should exceed 30°C and T_{air} min during nighttime should be higher than 20°C (according to the DWD definition for a tropical night, see section 2.1). Figure 7 shows minimum, maximum and mean air temperature for July 2006. Out of five days in July meeting this criteria, July 25th was picked as its 24-hour temperature and global radiation profile showed no abrupt changes, indicating absence of thunderstorms and cloudiness (see figure 8).
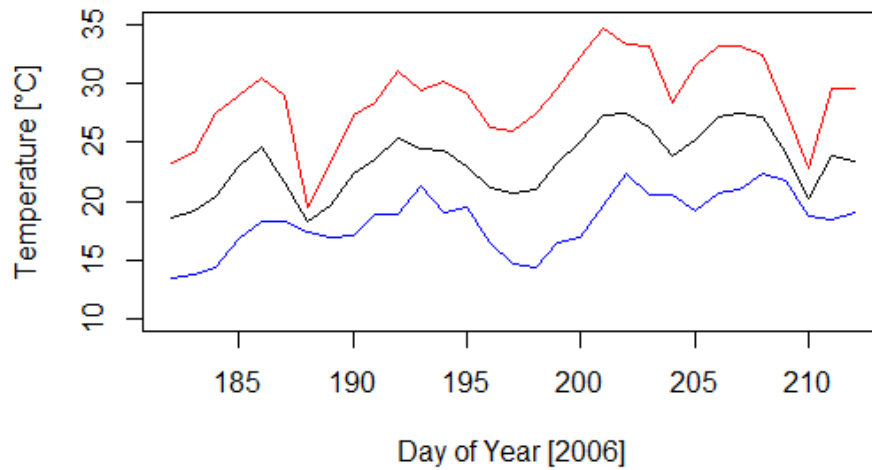
Figure 7: Temperature profile for July 2006, red= Tmax, black = Tmean and blue = Tmin (Data source: MIM 2016)
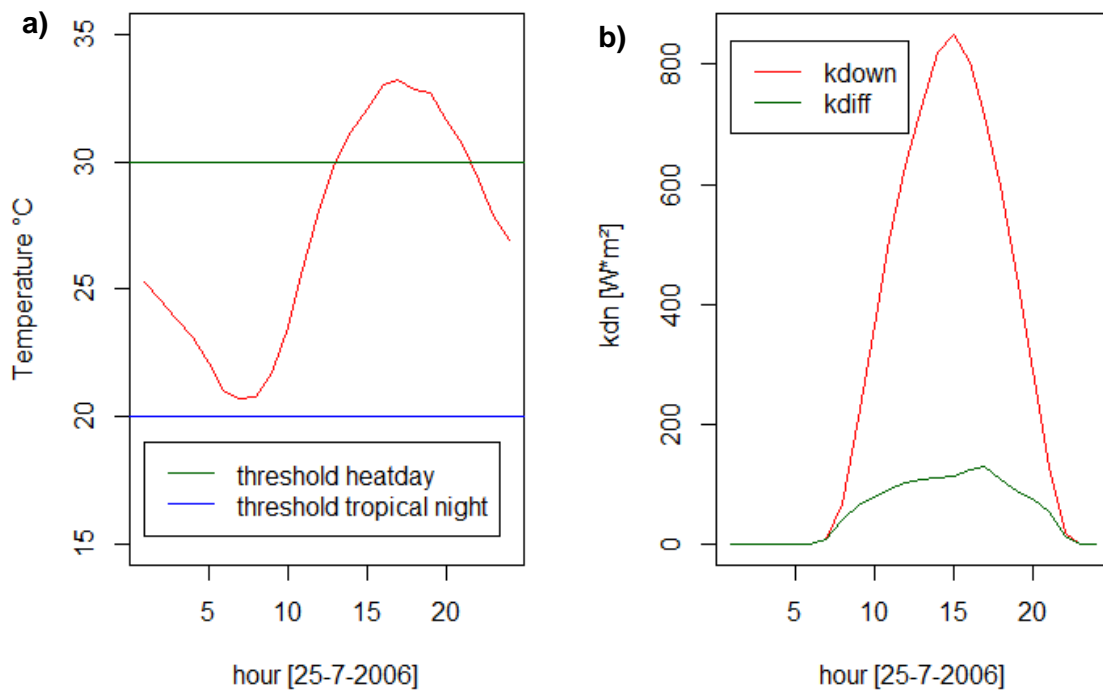
Figure 8: a) air temperature and b) global radiation profile for 25th July 2006

Since information on direct and diffuse radiation is not always provided by measuring stations, SOLWEIG offers the possibility to calculate both from global radiation data (Lindberg and Grimmond 2011). As data of diffuse radiation are available for the weather station Theresienstraße, the simulation was run twice, once with values calculated in SOLWEIG (test 1), once with complete input data (test 2), where direct radiation (k_{dir}) = global radiation (k_{dn}) – diffuse radiation (k_{diff}). The model runs differed in their result, such it was assumed that test 2 results are likely to be more precise since they are more directly based on measuring information. For k_{diff} calculation in SOLWEIG, a relatively simple empirical approach by Reindl et al. (1990) is applied (Jänicke et al., 2015). After pretests, the input DEMs were downscaled to 2m pixel size to significantly reduce computation time while yielding reasonably accurate results. SOLWEIG allows to modify urban parameters (albedo and emissivity), personal parameters (absorption and posture) as well as the geographical location. The geographical information was fitted to Munich, the rest was left as default as there was no reason to suggest otherwise. 24 hourly ascii-grids of skyview factor and T_{mrt}- distribution were gained and further analysed in R and ArcGIS. Since there is no T_{mrt} heat threshold adapted to Germany, Thorsson and colleagues' (2014) threshold of 55.5°C T_{mrt} for moderate heat stress is applied. In their study, this was the point where the number of death among elderly increased significantly. To deepen the analysis, two more heat levels are distinguished: 65-75°C is regarded as strong, temperatures above 75°C as extreme heat stress. In order to assess the influence of vegetation, an additional scenario without any trees or bushes was run for the same modeling day and compared with the original scenario.

Hazard assessment results were aggregated on city district part level as well as for Maxvorstadt's city structure types for refined analysis. A reviewed vector data set of Maxvorstadt was provided by the Centre for Urban Ecology and Climate Adaptation (ZSK). Visualisation and statistical analysis was performed in ArcGIS and R

3.2.2 Vulnerability assessment

As depicted in section 2.2, various approaches for creating a vulnerability index exist. However, according to several authors (Bradford et al., 2015; Johnson et al., 2012; Reid et al., 2009; Wolf et al., 2011) the most common indicators are the following: high age (older than 65), very high age (older than 75), very young (3 years or younger), single households (as a proxy for social isolation), single households older than 65 years, population density, low education (below high school degree), economic status (persons below poverty line), minority status or ability to speak the official language, lack of air conditioning and medical predisposition. While the first six indicators are available on city district part level, data such as education level, health and economic status are not provided by the city of Munich due to data privacy reasons. Availability of air

conditioning is not ascertained for Munich, but is also seen as less relevant in the European context if compared to the US (Johnson et al., 2012). Nevertheless, information about percentage of foreigners which is an equivalent to minority status and unemployment rates exist. The latter can be employed as a proxy for low income (Depietri et al., 2013). In order to acknowledge the influence of social cohesion, Chuang (2013) analysed unemployment and vacancy rates. While detailed vacancy rates are missing and less noteworthy for an inner city district of quick growing Munich, migration flux (influx and migration combined) was, similar to Chow et al., (2012), chosen as an indicator for neighbourhood stability. The less inhabitant fluctuation, the better chance for social ties to develop and maintain. These socioeconomic data were accessed for the city district parts from the city of Munich's indicator atlas (LH München, 2016) for the year 2015.

Biophysical influences are neglected by a large number of studies, yet their importance is not to underestimate, especially with respect to prevalence of vegetation (Ketterer and Matzarakis, 2014). As regard this study, vegetation is considered twice: Once as the amount of trees per CDP and once as the average distance to green areas per CDP. The amount of trees was calculated from the vegetation mask raster provided by the ZSK. If there is no or little vegetation in one's building block, a nearby park or little green space can provide a source of relief. Thus, the shorter the distance to the next vegetated area, the better options are provided for an individual to adapt to heat, which is why average distance to green was included as a further indicator. All parks and green spaces in Maxvorstadt and a buffer zone of 300m around it were digitalized based on the NDVI imagery. 300m is the distance defined by Natural England's Accessible Natural Greenspace (ANGSt) standards providing green is no more than a 5 min walk from home (Natural England, 2009). Thus, a total number of 166 green spaces were collected. Due to limited cooling and recreational potential, green spaces smaller than 0.5ha were excluded from further analysis. The distances to the 25 remaining green areas were assessed with the "Cost distance analysis" tool in ArcGIS, which calculates the most effective way from source to source based on a cost raster. Green spaces were selected as "sources" and buildings as "barriers", so that they have to be walked around. This constitutes an advantage over a simple buffer analysis which neglects obstacles and thus underestimates walking distances. Statistics for each CDP were calculated using the Zonal Statistics Tool in ArcGIS. Table 2 shows an overview of all selected vulnerability indicators.

Table 2: Overview of the eleven vulnerability indicators

no.	indicator	unit	source
	Socio-economic		
1	Very young (<3)	%	Indicator atlas Munich 2015
2	High age (65+)	%	Indicator atlas Munich 2015
3	Very high age (75+)	%	Indicator atlas Munich 2015
4	unemployed	%	Indicator atlas Munich 2015
5	foreigners	%	Indicator atlas Munich 2015
6	fluctuation	EW/1000 EW	Indicator atlas Munich 2015
7	Single hh	%	Indicator atlas Munich 2015
8	Single hh 65+	%	Indicator atlas Munich 2015
9	Population density	EW/km²	Indicator atlas Munich 2015
	Built environment		
10	Amount of vegetation	%	GIS analysis, vegetation mask
11	Average distance to green area	meter	GIS analysis, NDVI image 2013

Due to absence of absolute thresholds for each indicator, relative thresholds were employed for assessing the intensity of each indicator. In order to do so, all indicator values were normalized having a mean of 0 and a standard deviation of 1:

$$x_n = (x_i - \bar{x})/sd$$

where x_n = normalized indicator value,

x_i = original indicator value,

$\bar{x}$ = mean of indicator x and

sd = standard deviation of indicator x.

This normalization has the advantage that the same vulnerability scala can be applied to all indicators, based on fixed standard deviation units. The resulting factor score was divided into six equal increments of ± 1.0 SD and assigned integer values from 1 (≥ 2 SD below mean) to 6 (≥ 2 SD above mean) (see also Harlan et al., 2006; Reid et al., 2009), where 1 represents very low and 6 very high peculiarity (see table 3).

Table 3: Scale for vulnerability indicators according to standard deviation units. Values ± 1.0 correspond medium, <-1 low and very low, >1 high and very high vulnerability

scala	1	2	3	4	5	6
Norm. ind.	-2.9 – (-2)	-1.9 – (-1)	-0.9 - 0	0.01 – 0.9	1 – 1.9	2 – 2.9
expression	very low	low	low – medium	medium - high	high	very high

Given there is no further information about mutual influence between the indicators, standardization and unweighted quantitative aggregation represents a common approach in vulnerability index composition (Bao et al., 2015; Chow et al., 2012). Thus each CDP's vulnerability index was gained by aggregating the eleven indicator scores for each CDP:

$$V_{cdp} = \sum vi / n_{vi}$$

where V_{cdp}= *vulnerability index for each CDP,*

vi = vulnerability indicator,

n = quantity of vi.

3.2.3   Risk assessment

In order to produce the final risk map, the vulnerability layer and the hazard layer are combined, by multiplication (Krüger et al., 2014; Dugord et al., 2014):

$$R_{cdp} = H_{cdp} * V_{cdp}$$

 where R_{CDP} = *risk index for each CDP,*

H_{CDP} = *hazard per CDP,*

V_{CDP} = *vulnerability index for each CDP.*

For improved clarity and understanding, the layer's values are transferred to a scala from low to very high, pursuant to their classification in percentiles (see table 4).

Table 4: Risk scale for heat according to percentiles

risk level	low	medium	high	very high
percentile	<50%	50-75%	75-95%	>95%

In order to assess the risk for vulnerable social infrastructure locations of retirement homes, kindergardens schools and museums were mapped with help of the business directory Munich (Portal München, 2016c) and other supporting sites (e.g. Gelbe Seiten, das Örtliche) since no official complete list exists.

4   Results

4.1   Heat stress assessment

Figure 9 shows the 24 hour course of T_{mrt} for Maxvorstadt based on structure type units. Several observations can be made: From 6am to 10pm the curve resembles a normal distribution with a peak in the early afternoon. Thus, the highest heat stress is to expect around 2pm. The lowest T_{mrt} values are detected for 5am and increase more rapidly in the morning than they decline in the evening. Interestingly, the variability of T_{mrt} values is highest during hours with advanced amounts and lowest at 6am, 7am and 8pm. Hence, thermal properties are most uniform during these hours, while differences of as much as 20°C are notable between 11am and 6pm.
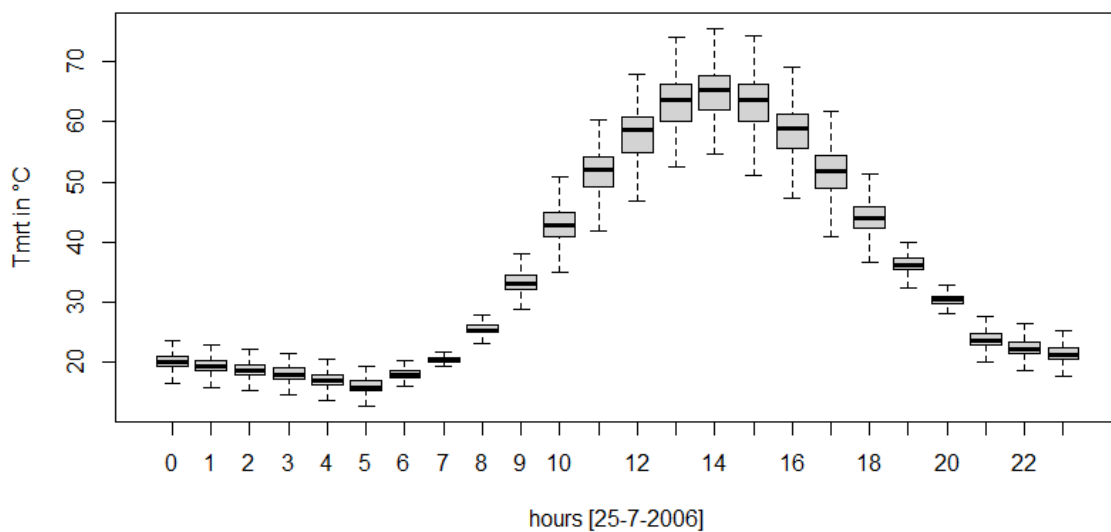
Figure 9: T_{mrt} over 24hrs for 25th July 2006, aggregated on urban structure type level

If the model results for 2 x 2m resolution are considered, until 10 am in the morning and after 10 pm in the evening, there is no place where the T_{mrt} values exceed 55°C. At 10 am – 11 am, 11% of Maxvorstadt experience moderate heat stress (T_{mrt} between 55-65°C). From then on, the area share above the heat threshold increases rapidly: While it is already more than half of the area (55%) at 11pm, it amounts to 68% at 2 pm. Then, 10% of Maxvorstadt experience moderate heat stress, whilst 58% is even above 75°C T_{mrt}, which is understood as extreme heat stress in this analysis. The most severe heat stress is observed from 1 pm to 4 pm, with a significant share exceeding 75°C. Interestingly, there is also a relatively sharp divide between hotter and cooler areas, since temperatures tend to either fall below 55°C or pass beyond 75°C, while only 10% of the area has values inbetween. At 6 pm, 70% of the area are below the heat threshold again (see also Figure 12).

Figure 10 depicts the spatial distribution of T_{mrt} loads at 2-3 pm. This is not only the hour with the most extreme T_{mrt} values, but also with the greatest divide between cooler and hotter areas.

A majority of the streets in Maxvorstadt follow an orthogonal scheme with slightly NNE-SSW and NSW-SNE running streets. For easier communication these will be labeled as N-S and E-W running streets respectively. Areas below the heat threshold (up to 55°C) are marked in blue on the map, areas well above the threshold (75°C-85°C) appear in red. There is almost no place that falls between these two extremes: Solely the top building edges show values between 55-75°C T_{mrt}. While open spaces and N-S running streets carry the highest heat loads, E-W running streets, narrow inner court yards, sites under trees and on the north side of buildings are significantly cooler than their surroundings.
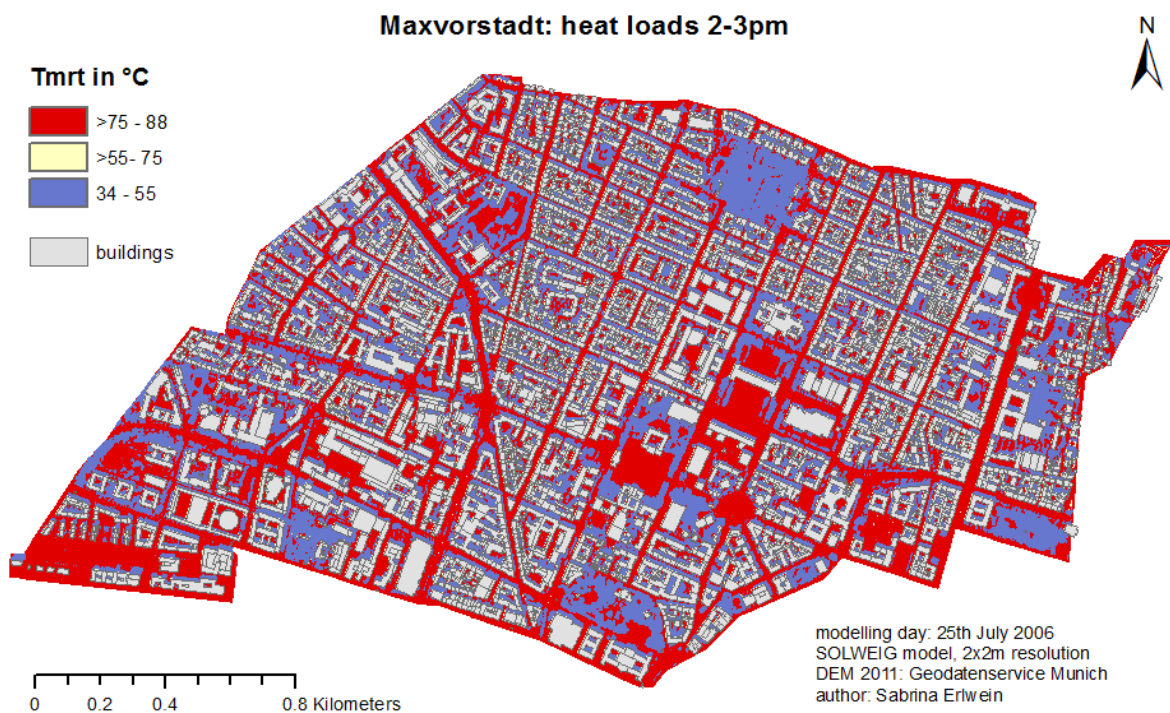
Figure 10: Tmrt [°C] distribution from 2-3pm, all areas under the heat stress threshold of 55°C T_{mrt} are blue, above yellow and red, resolution size is 2m x 2m

This spatial pattern is representative for hours with high heat stress, whilst derivations occur in the early morning and late evening hours. Until 8am in the morning tree-covered sites appear to be warmer than unvegetated ones. Areas in the south and east of buildings are cooler than adjacent sites. At 11 am the east of the buildings is shaded, thus narrow (up to 18m) N-S running streets have low T_{mrt} values. From 8pm in the evening, open spaces and roof tops cool down quickly, so that from 9pm onwards their heatloads are smaller than of tree-covered sites.

In general, orientation and width are decisive factors for street heat loads. Rather narrow streets as for example Türkenstraße are cooler than broad ones except for the early morning and late evening hours. Broad N-S running streets (e.g. Ludwigstraße) are warmer in the morning, but cooler during midday and the late afternoon than vast E-W oriented (e.g. Nymphenburgerstraße). Since the main focus of this work is on heat stress, the spatial

25

distribution of T_{mrt} values from 2-3 pm was taken as an indicator despite these temporal changes. T_{mrt} from 2-3 pm nevertheless correlates strongly with the T_{mrt} average over 24 hours ($r = 0.94**$).

4.1.1   Influence of vegetation

To better understand the influence of vegetation, a simulation of with the same meteorological input data but without any greenery was run. Figure 11 depicts minimum, maximum and mean T_{mrt} values over 24 hours for the original settings and the new scenario. It is shown that minimum and maximum T_{mrt} values are nearly identical, while the total average is 2°C higher than in the original scenario. From 10 am and to 6 pm, the hours with the highest heat loads, the unvegetated average is distinctly higher. As regards the late evening and early morning hours the opposite is true.
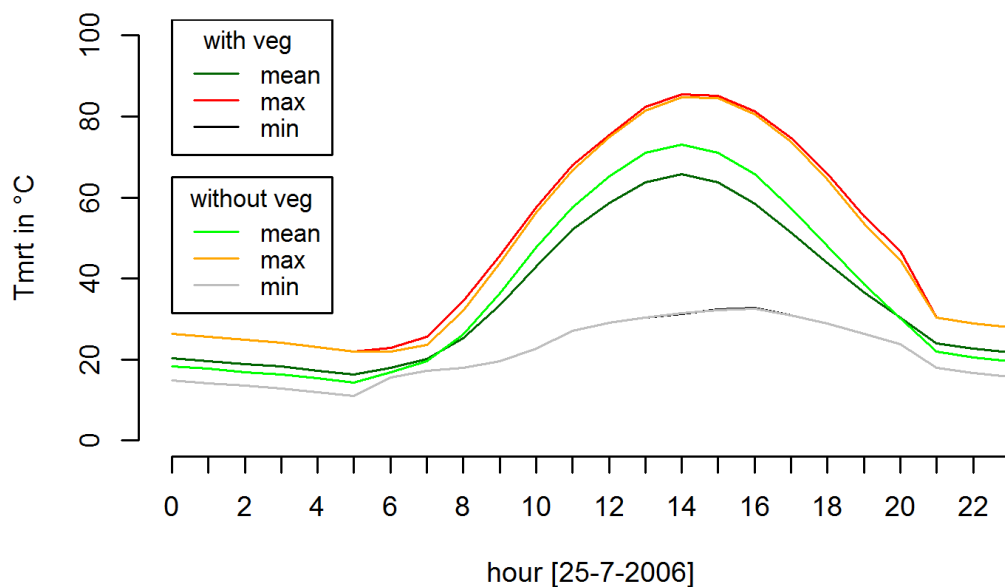
Figure 11: Comparison of minimum, mean and maximum Tmrt values for vegetated and unvegetated scenario over 24 hrs

Analysing spatial-temporal differences, it can be stated that in the scenario without greenery, Maxvorstadt heats up more quickly and cools downs faster. On the other hand, a greater proportion of the area is affected by heatstress if all vegetation is removed (see figure 12 next page). While in the original setting, 55% is affected by heat stress at 11am, it is 73% without vegetation. At 2 pm, 86% of the area exceeds the heat threshold of 55°C T_{mrt} instead of 68% in the original scenario. Notably, the percentage of area under extreme heat stress (more than 75°C) increases from 58% to 75%.
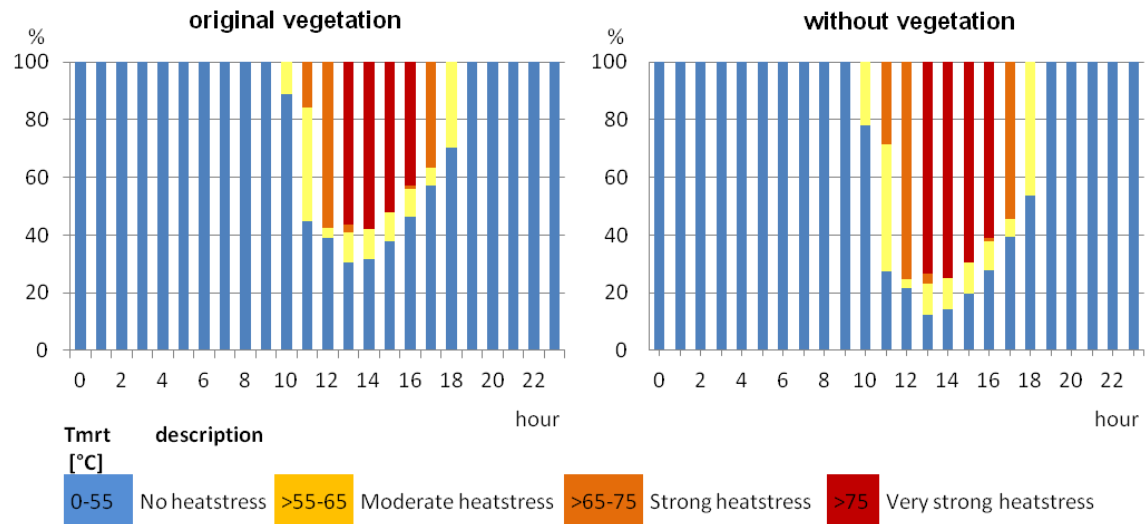
Figure 12: Comparison of areas under heat stress for vegetated and unvegetated scenario over 24hrs
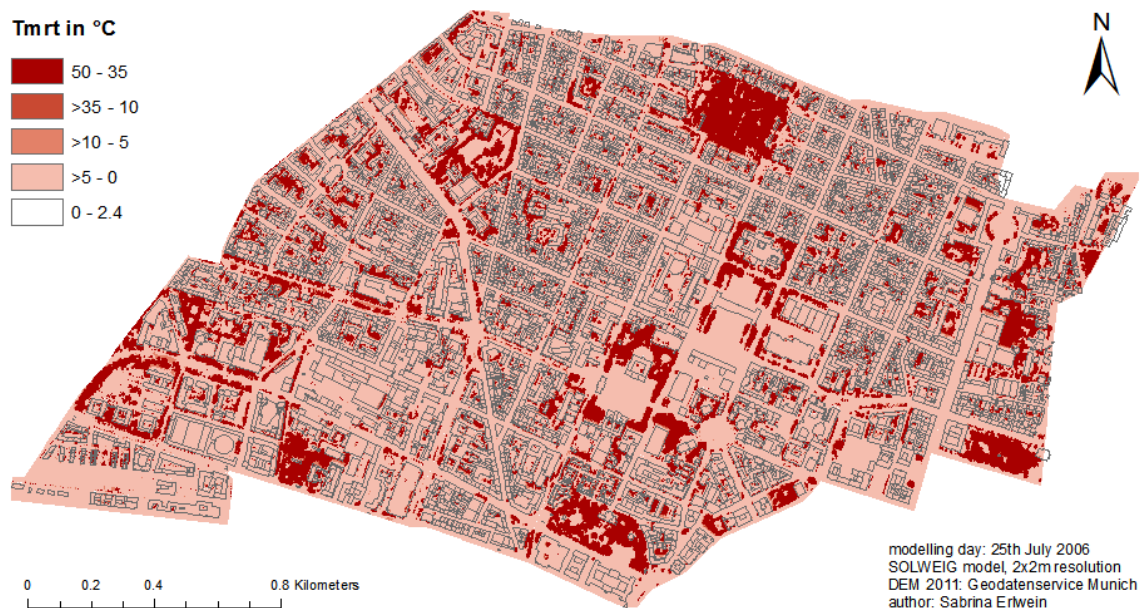
Figure 13: Differences between T_{mrt} during 2-3 pm with and without vegetation. The darker the red, the higher the T_{mrt} values compared to the scenario with vegetation

Figure 13 highlights the areas with differences in T_{mrt} between the two scenarios. Sites were where T_{mrt} values of the simulation without greenery exceed those of the original one are marked in red. The darker the red, the higher the T_{mrt} values. A very slight increase of temperature levels (0-5°C T_{mrt}) is observed for the total of Maxvorstadt. At the location of bushes and trees in the original setting, temperature differences add up to as much as 50°C, showing that greenery has

a significant impact on T_{mrt} values. For better understanding the influence of various urban parameters, characteristics of urban structure types and their impact on mean radiant temperature were analysed in the following.

4.1.2   Influence of urban geometry and urban structure

Twenty different urban structure types, distinguishing different building types, linear structures and categories for green and open spaces, are recorded for Maxvorstadt. For each structure type, percentages of sealed, vegetated and built surface for its units and their size were aggregated and displayed as fractions of the total area of Maxvorstadt (see table 6 in the appendix). As there is no information on green coverage rates of streets given (e.g. through street trees), the respective fields are left blank. As much as 80% of Maxvorstadt is sealed, buildings and streets occupy 41% respectively 23% of all surfaces. Vegetation covers 25% of the area – since the data is derived from aerial images and e.g. tree crowns extend into their surrounding surfaces, sealed and vegetation covered surfaces add up to more than 100%. Overall, Maxvorstadt's urban structure can be described as rather homogenous (see figure 14). Perimeter building blocks are the prevailing structure type, being present on 45% of the total area, followed by large storey buildings (13%). Parks, avenues and green areas only make up 7% of the area and contribute less than 50% to the total greenery. A large amount of vegetated surface is instead entailed in perimeter building type units, providing 41% of the total vegetation amount.

Urban structure types Maxvorstadt

perimeter building	high rise buildings	large avenue	roads
perimeter development	linear development	park	
mixed multi-storey buildings	chain building	small green space	
large storey building	special construtions	open spaces	
small storey building	mixed development	small detached buildings	

0   0.2   0.4   0.8 Kilometers

Data source: ZSK, 2016
State of data: 2011
EPSG: 4126
Author: Sabrina Erlwein

Figure 14: Map of urban structure types in Maxvorstadt

However, structure type units differ among each other, there are no characteristic fractions of greenery and sealing for each structure type observable. Such, perimeter building blocks vary in their vegetation amount between 0% and 53%. Even structure type "small green spaces" varies between 100% and 53% vegetation coverage. Figure 15a shows the correlation between heat load at 2 pm and vegetation amount for all blocks. Streets were excluded from the analysis, since their vegetation percentages were not recorded. Generally, T_{mrt} at 2 pm and vegetation cover are moderately negatively correlated (r=-0.63**). The data suggest that for remaining under the heat threshold (dashed line) during the main heat stress hour, an area has to be at least 50% vegetated. Notably, the deviation between T_{mrt} values expands with increasing vegetation coverage. Units with 90% vegetation coverage or more differ between 38°C and 82°C T_{mrt}. Especially the structure type "small green areas" (highlighted in green) shows a very wide spread. Excluding this structure type (21 areas), the deviation is distinctly reduced (r= -0.73**) and a linear trend is observable (figure 15b). Maxstadt's main structure type, perimeter buildings (marked in blue), concentrates in the left upper half of the scatterplot and is more homogenous than small green spaces (r=-0.7**, n=125). Since all other structure types are only represented in low quantity (n=1-20) further correlation analysis for each type was not regarded as meaningful.
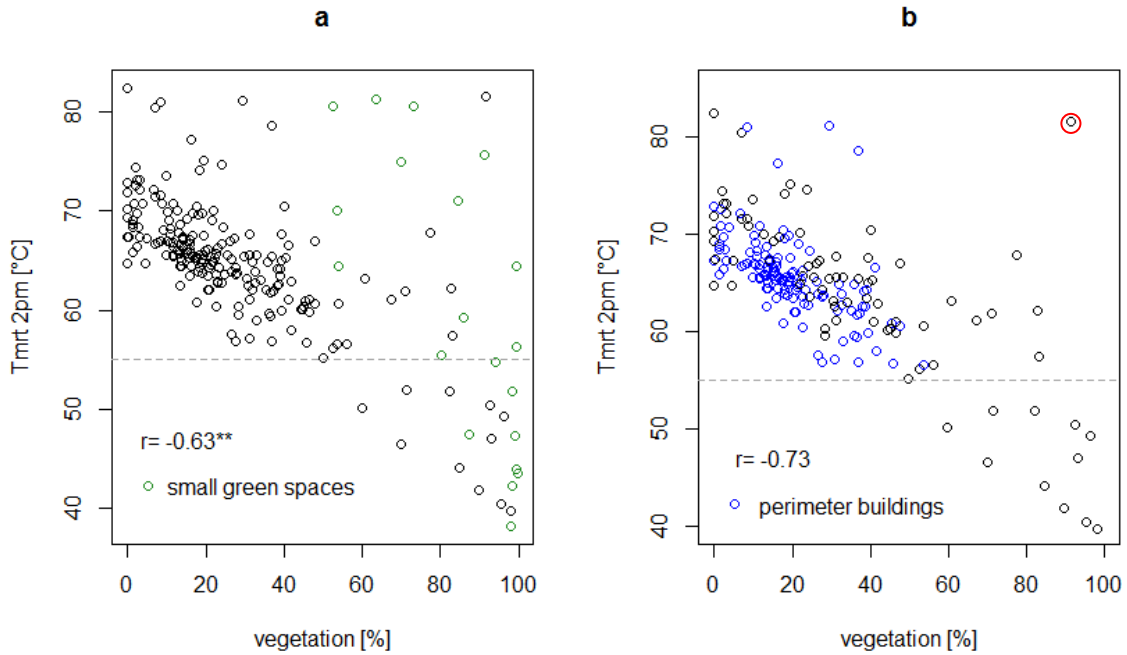
Figure 15: Correlation between T_{mrt} at 2-3 pm and vegetation amount for a) all urban structure type units (n=222), and b) without type "small green spaces" (n=201), outlier marked in red

Figure 16 shows the diversity of small green spaces regarding type (traffic island, lawn) and vegetation cover. The red-marked outlier of figure 15b is a grass patch located next to a main road with a vegetation cover of 92% (see figure 16b). Yet, compared to the small green space densely covered with trees in picture 16a, T_{mrt} at 2 pm is as much as 44°C higher. Moreover, without the shade of adjacent buildings and trees it has one of the highest heat loads of all structure type units.

veg 70%	veg 98%	veg 63%	veg 92%
Tmrt 75°C	Tmrt 38.2°C	Tmrt 81.3°C	Tmrt 82°C
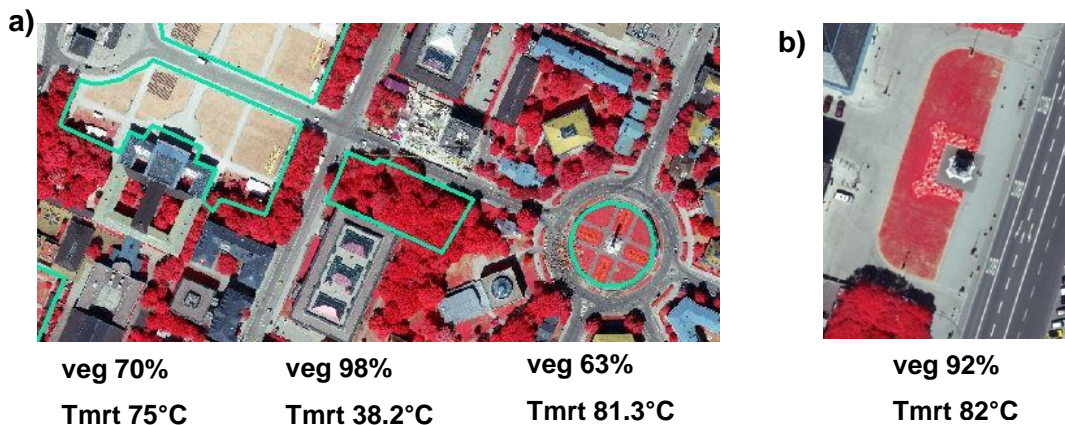
Figure 16: Examples of small green spaces with a) different amount and type of vegetation cover and b) open space with high vegetation cover and high T_{mrt} value

Considering all structure type units, the highest heat loads at 2pm are registered for open, sunlit areas, whereas the lowest T_{mrt} values are found in parks with dense tree cover (see figure 17).
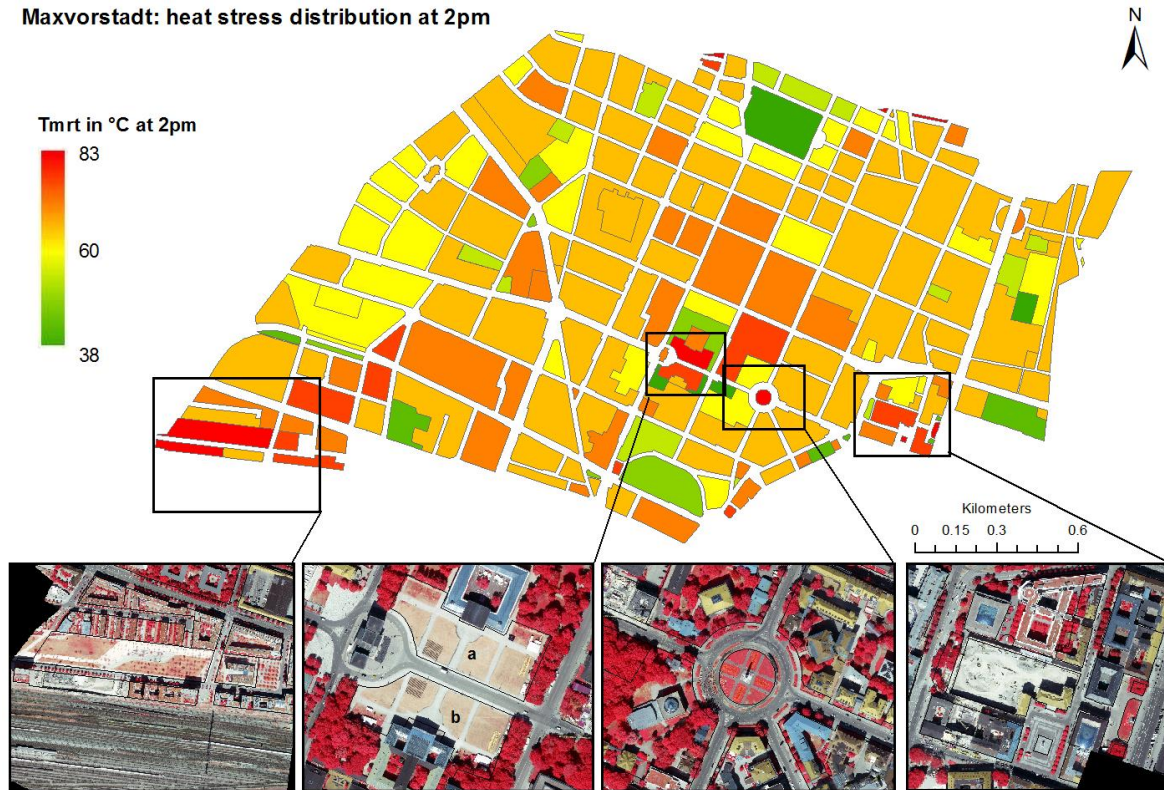
Figure 17: T$_{mrt}$ distribution during 2-3 pm for Maxvorstadt on urban structure type level (source of pictures: Geodatenservice München, 2013)

It is also shown that characteristics of the surrounding environment have a significant influence: The north side of Königsplatz (a, second picture) has a mean heat load of 81°C T$_{mrt}$ at 2 pm compared to an average of 75°C T$_{mrt}$ for the southern side (b). While parts of site (b) are shaded from the sun by building and vegetation located in the south of the area, trees located in the north of site (a) don't provide shade to the site during midday and afternoon, which represent the hours with the highest heat loads.

For closer analysis of the influence of different site characteristics on Tmrt over the day, five sites with different skyviewfactors and vegetation coverage were selected (figure 18). Site 1, located in the former graveyard "Alter nördlicher Friedhof", is densely covered with trees. Site 2, Königsplatz, represents a grass covered open space. Site 3 to 5 are perimeter building blocks with low (3%), medium (20%) and high (48%) vegetation coverage. For all sites, the lowest mean value is observed at 5am and the highest mean value at 2 pm. Remarkably, the difference between the lowest and the highest mean value for site 2 (T$_{mrt}$ 12°C to 81°C) is nearly four times greater than for site 1 (T$_{mrt}$ 22 to 39°C). Thus, temperature differences over the day are considerably more extreme for the open space and also the perimeter building blocks than the tree-covered site. While T$_{mrt}$ values of site 1 never exceed the heat stress threshold of 55°C, site 2 is under heat stress from 10 am to 7 pm. The perimeter building blocks with high and medium vegetation amount reveal slightly higher heat loads than the site with low vegetation coverage.

Notably, during nighttime this order is turned upside-down: Thus, until 7 am in the morning and from 8 pm in the afternoon the tree covered space has higher T_{mrt} values than all other sites, while the opposite holds true for the open space. Inspite of significant differences in vegetation coverage, T_{mrt} values of the perimeter building blocks are relatively similar to each other. Regardless of the vegetation amount, low skyviewfactors are caused by the characteristic perimeter building structure with high buildings at the rim of the block. The inner court yards of site 3 to 5 are either filled up with trees and bushes (site 5) or several smaller buildings and such more or less equally shaded. Nevertheless, a T_{mrt} reduction of 7°C is visible for site 5 with high tree cover compared to concrete dominated site 3.
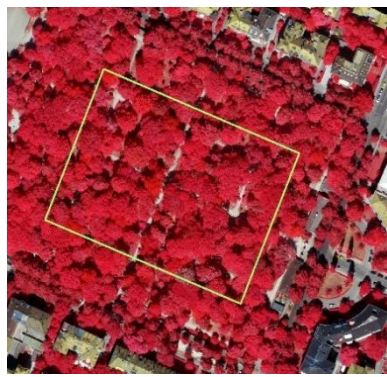
site 1 park (veg 98%)　　　　site 2 open space (veg 70%)

site 4 (veg 3%)　　　　site 5 (veg 20%)　　　　site 5 (veg 48%)
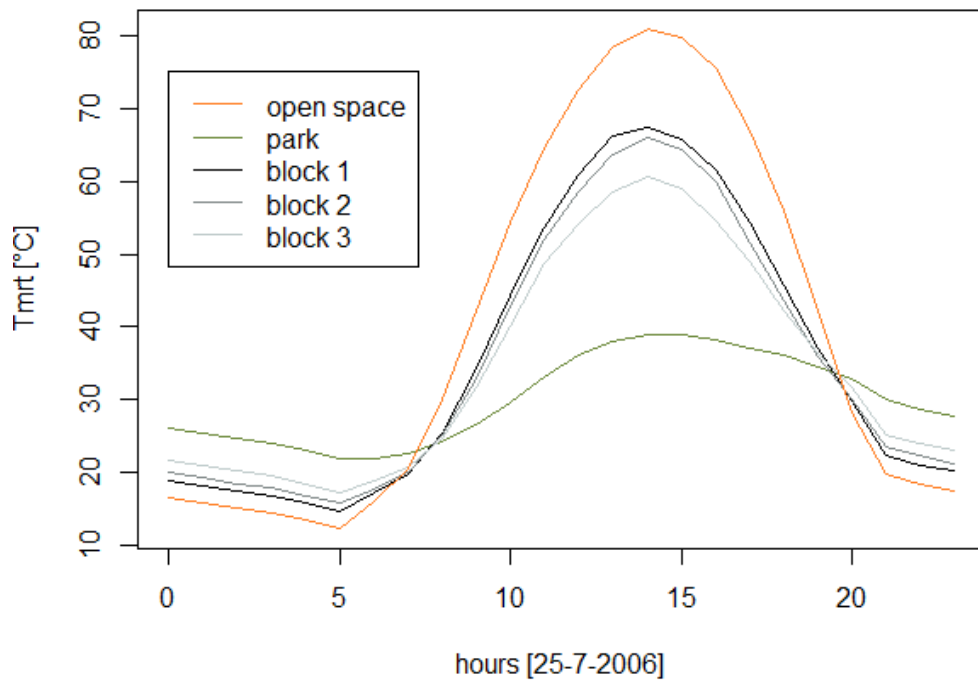
Figure 18: T$_{mrt}$ values over 24hrs for an open space, a tree covered park and three perimeter building blocks with different vegetation amounts (3%-20%-48%) (picture source: Geodatenservice München, 2013)

4.2   Heat risk assessment for city district parts

4.2.1   Hazard analysis

To compare heat loads, hourly mean T_{mrt} scores of each city district part were plotted for 25th July 2006 (see figure 19). Since the meteorological input remains the same, all curves show the same course over the day, with a minimum at 5 am and maximum at 2 pm. While T_{mrt} values are nearly identical from 6 am to 10 am and 8 pm to 9 pm, differences are visible in the late evening and early morning hours and increase steadily with increasing radiation and air temperature in the early afternoon. At 2pm, the gap between the highest (70.5°C, Marsfeld) and the lowest (61.5°C, Am alten nördlichen Friedhof) T_{mrt} value amounts to 9°C.
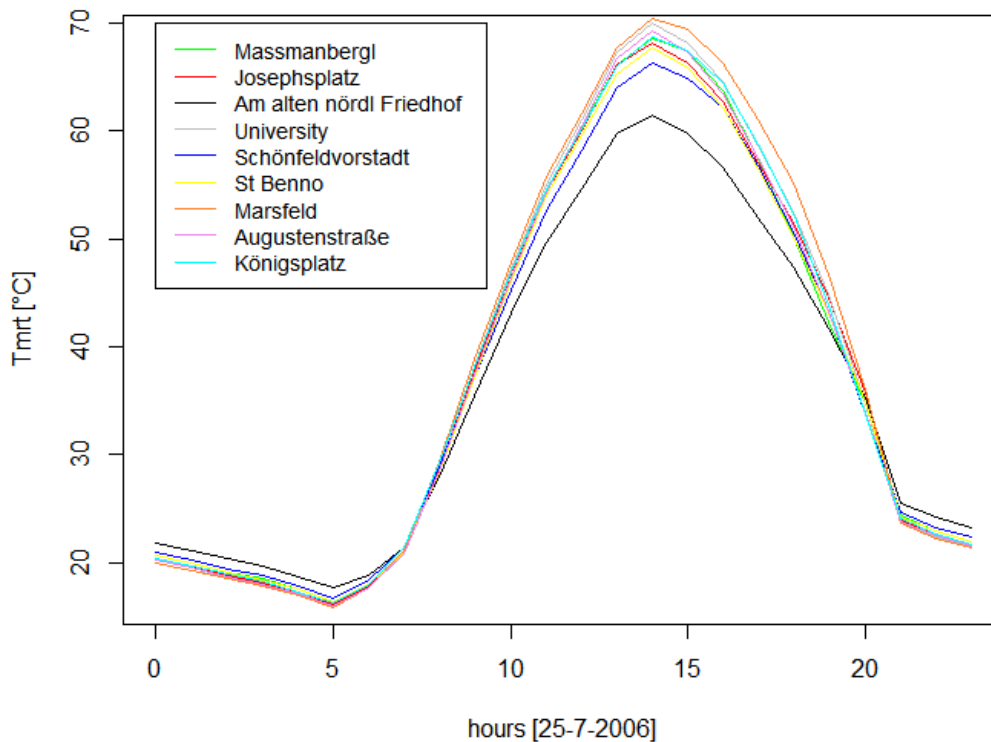
Figure 19: Comparison of T_{mrt} over 24hrs for Maxvorstadt's city district parts

Seen across the day, Marsfeld and University are the city districts parts with the highest average heat loads, while the least heat stress is assessed for the areal "Am alten nördlichen Friedhof". Interestingly, during hours with no or little global radiation (9 pm to 6 am), the coolest CDPs during the day appear to be the warmest and vice versa. Such, "Am alten nördlichen Friedhof 's" average is 2°C higher than "Marsfeld's" during that time period.

4.2.2 Physical environment: amount of green and distance to parks

The amount of vegetation per city district part was analysed on basis of a vegetation raster provided by the ZSK which was derived from satellite imagery (year 2013). A quick validation of the raster revealed an overall good match, except for two cases: Firstly, detection of especially larger grass areas was problematic, such e.g. Königsplatz and Arnulfplatz were missing in the dataset. Secondly, green roofs can be misspecified as trees, since vegetation is classified according to height, however this happened only in very few cases. The amount of grass was corrected by manually editing large lawns. Figure 20 compares shares of trees, bushes and grass of the city district parts. While the most vegetation is found in CDP "Am alten nördlichen Friedhof" (38%), "Universität" (17.5%), "Augustenstraße" (17.5%) and "Josephsplatz" (19%) have the least vegetation shares. Overall, the higher the amount of total vegetation, the higher the amount of trees. Only Augustenstraße has a slightly higher tree amount than Universität despite its lower vegetation coverage. Trees dominate in all city district parts (13-34%), followed by grass (1.5-8.2%) and bushes (1.6-3%). However amount of bushes and grass is underestimated since vegetation and ground cover below trees are not recorded. Due to this and the fact that the most important cooling impact of vegetation is provided by shading (Jänicke et al., 2015; Mayer, 1993), tree amount instead of vegetation amount is used as a vulnerability indicator.
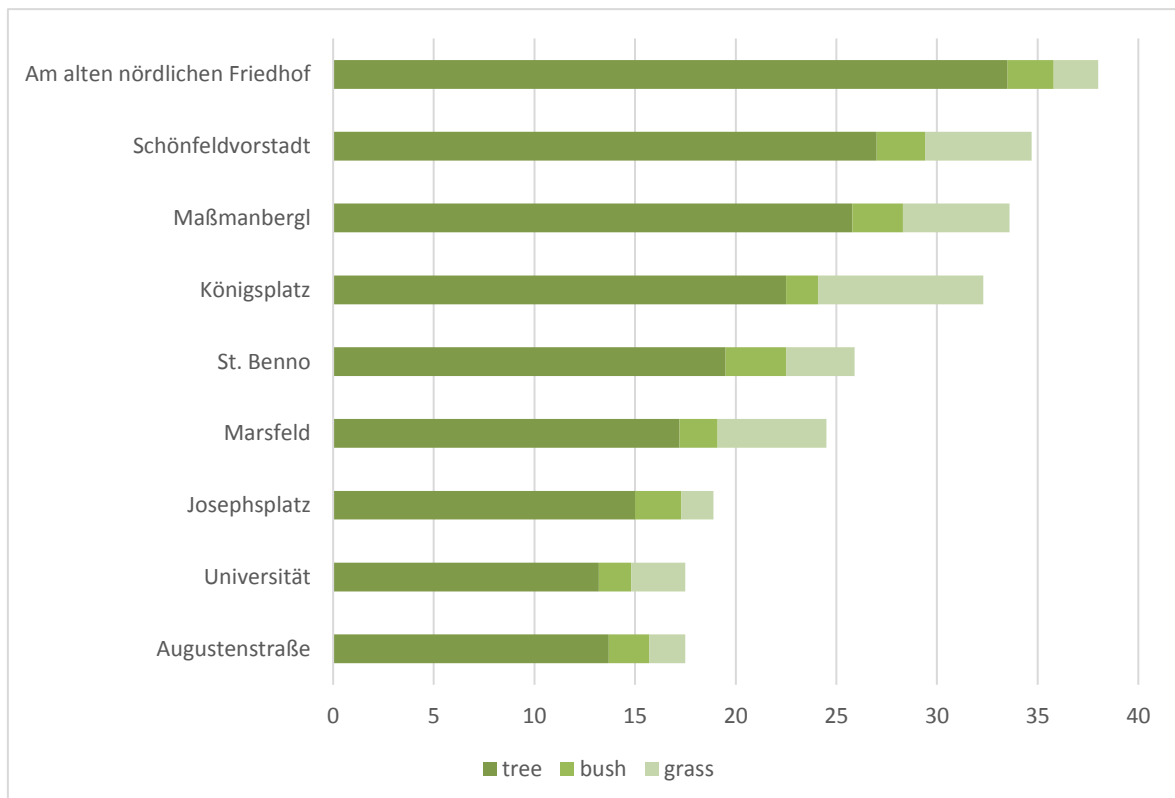
Figure 20: Amount of trees, bushes and grass for each city district part

While this analysis provides a first impression concerning the green environment, green space distribution within CDPs, their location, size and patterns are not considered. For this reason,

an additional, geographically more explicit analysis was performed to assess mean distances to green spaces. As described in section 4.2.2, green spaces were considered if they had a minimum size of 0.5ha, were located in Maxvorstadt or a buffer zone of 300m and were covered with trees. Such, single trees and patches of grass were not recorded. In Maxvorstadt, 19 green spaces larger than 0.5ha exist, half of them being smaller than 1ha (table 3). Tiny green patches contribute a remarkable amount to total green space, also because larger parks are rare in the inner city district.

Table 3: Size and number of treed green spaces in Maxvorstadt

Size	count	area (ha)	% area
0,2 bis 0,5 ha	142	20	39%
0,5ha bis 1ha	10	7,5	15%
1ha bis 2ha	3	4,7	9%
2ha bis 3 ha	2	4,3	8%
3ha bis 5 ha	4	15	29%

The largest greenspace in Maxvorstadt (4,5ha) is the former graveyard and name giver for its city district part "Alter nördlicher Friedhof", which is today used as a park. The old botanic garden in the south (CDP: Königsplatz) is the second largest one (3,8ha), followed by Maßmannpark (CDP: Maßmannbergl, 3,2ha) in the northwest of the city district. The Englischer Garten, Munich largest park, borders to Schönfeldvorstadt in the east, but is not within the margins of Maxvorstadt. In its south, the Hofgarten, a Court Garden of 6,5ha, is located. Only smaller green spaces can be found in the city district parts Universität, Josephsplatz, Augustenstraße and St.Benno. Figure 21 depicts the location of and walking distances to the analysed green spaces and parks.

Maxvorstadt: Distance to parks and green spaces

Distance in meters
- 0 - 300
- >300 - 500
- >500 - 750

1 = Maßmannbergl
2 = Josephsplatz
3 = Am alten nördlichen Friedhof
4 = Universität

5 = Schönfeldvorstadt
6 = St. Benno
7 = Marsfeld
8 = Augustenstraße
9 = Königsplatz

green areas > 0.5 ha

0   0.175   0.35   0.7   Kilometers
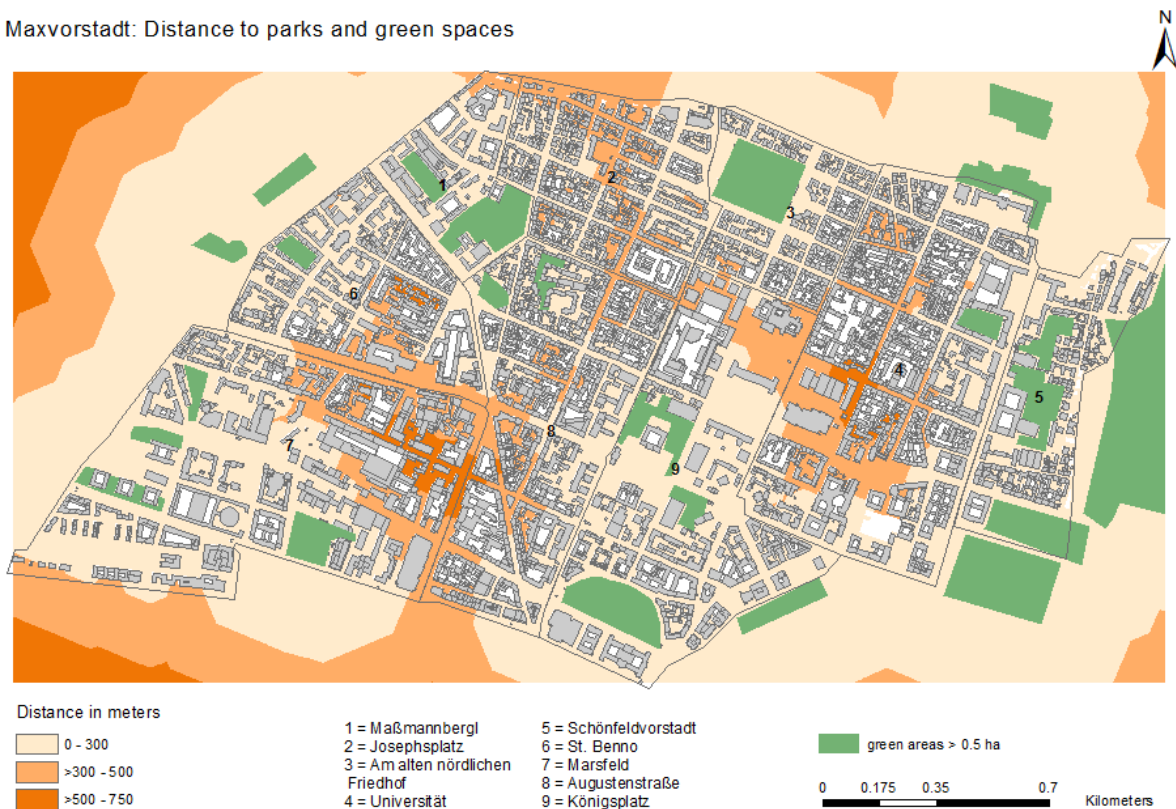
Figure 21: Map of walking distances to parks and green spaces with trees >0.5ha

For the whole of Maxvorstadt, walking distance averages to 240 m (sd = 143.2 m). The shortest mean distance (71m) is observed for CDP Schönfeldvorstadt (5), while walking distance is more than fourfold (308m) for CDP University, which has no bigger park with trees within its margins. Here and in Marsfeld are the largest deficit areas, where green areas larger than 0.5 ha are more than 500m away. Overall, despite the rather strict selecting criteria for the inclusion of parks, not many deficit areas are visible.

Figure 22 compares mean walking distances (orange line) for each city district part with its vegetation coverage (green columns). Though walking distances tend to become shorter with increasing vegetation coverage, there is no distinct relation between these two parameters. While vegetation coverage provides information about the greenery on site, walking distances also consider green spaces in adjacent neighbourhoods. Schönfeldvorstadt has a lower vegetation fraction than Am alten nördlichen Friedhof, but has a lower mean walking distance since it neighbours Munich's largest park "Englischer Garten".
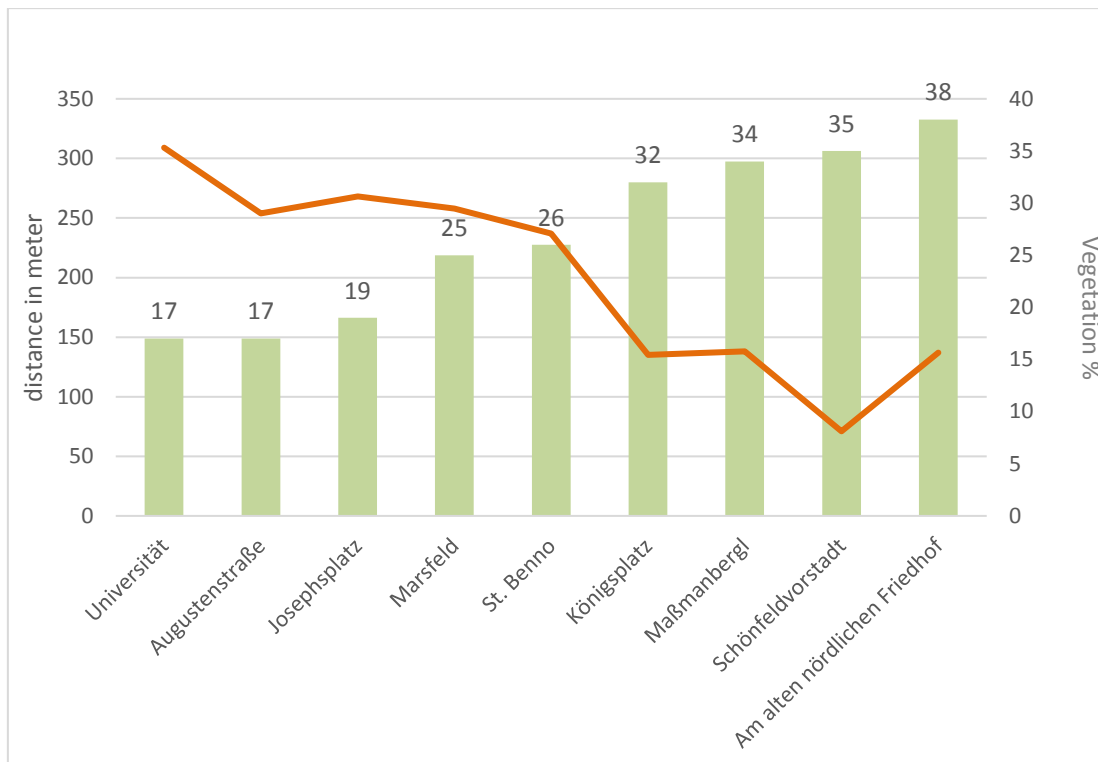
Figure 22: Comparison of walking distances (orange line) and vegetation coverage (green columns) for each CDP

4.2.3 Socio-economic vulnerability

Nine socio-economic indicators were selected to be part of the vulnerability index. Figure 23 depicts all indicators for each city district part after standardization and translation into a vulnerability score ranging from 1 to 6 (see also section 3.2.2). While high values represents high vulnerability and vice versa, it is important to acknowledge that in absence of absolute thresholds, these vulnerability levels are not absolute, but in relation to the other city district parts in Maxvorstadt. As an example, relative to Maxvorstadt, district part "Am alten nördlichen Friedhof" has high percentage of people above 74 years (7.3% compared to an average of 5.3%), which is why it gets a high vulnerability score. Yet, its share of very old people is still below Munich's average of 8.2%. Such, if the whole of Munich would be considered, the corresponding vulnerability score would rather be medium to low. On the other hand, Königsplatz, has not only a very high number of unemployed for Maxvorstadt (7.4% compared to a mean of 3.1%), but also as regards Munich (3.9%). For better overview, each indicator is depicted on a map, providing also the corresponding average for Munich (see figure 24).

38
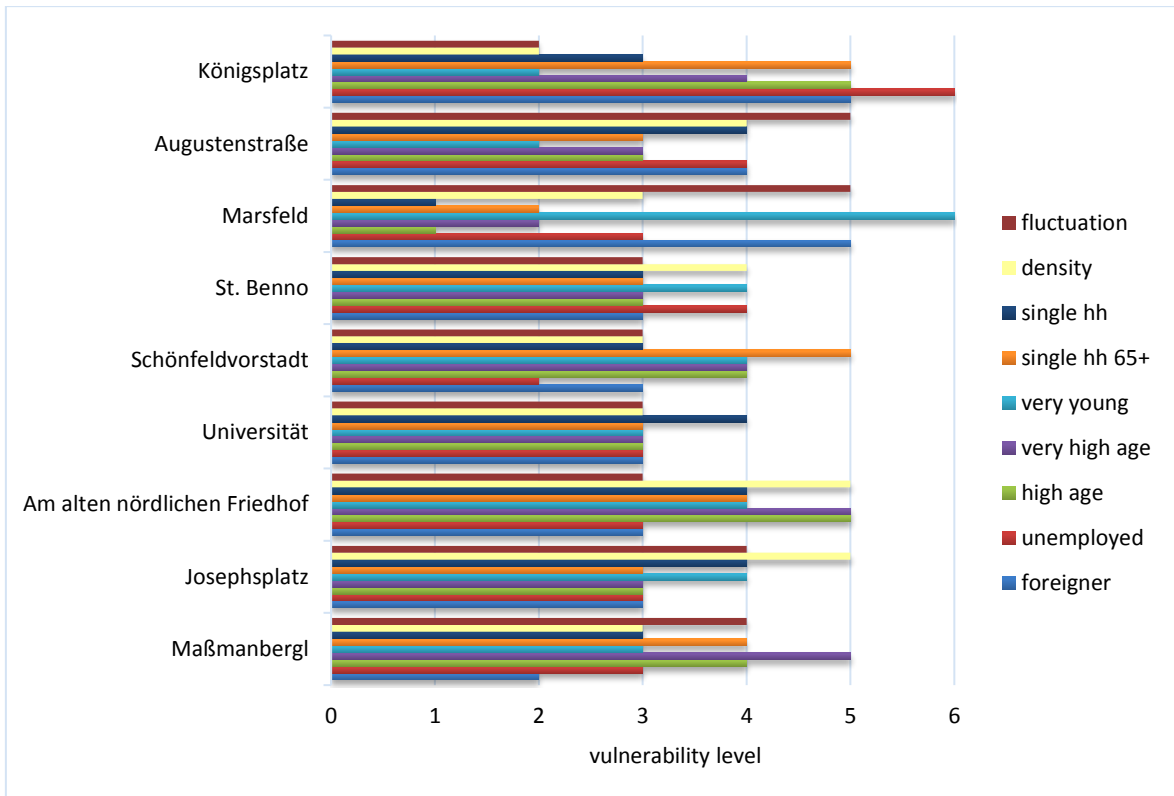
Figure 23: Vulnerability levels of socio-economic indicators for each CDP; values from 1 to six represent the vulnerability scala: 1=very low, 2=low, 3-4=medium, 5= high, 6= very high

Relative to Maxvorstadt, Marsfeld has a high number of young children, but on the other hand fewer than average single households (56% to 67%). Am alten nördlichen Friedhof and Josephsplatz are the most densely populated district parts, while the highest fluctuation of inhabitants occurs in Marsfeld and Augustenstraße. Schönfeldvorstadt and Königsplatz have the highest proportion of elderly living alone. Taken all socio-economic indicators, Am alten nördlichen Friedhof shows the highest and Universität the lowest vulnerability level.

Fluctuation (per 1000EW)
- 291 - 333
- >333 - 375
- >375 - 415
- >415 - 455
- >455 - 498

Munich: 301

Population density (EW per km²)
- 1187 - 7100
- 7101 - 13000
- 13001 - 18900
- 18901 - 24800
- 24801 - 30767

Munich: 4798

high age (>64, %)
- 6 - 7
- 8 - 9
- 10 - 11
- 12 - 13
- 14 - 15

Munich: 17.6

very young (<4, %)
- 1.9 - 2.3
- >2.3 - 2.7
- >2.7 - 3.1
- >3.1 - 3.5
- >3.5 - 3.8

Munich: 3

foreigner (%)
- 13 - 17
- 18 - 23
- 24 - 29
- 30 - 35
- 36 - 44

Munich: 26

very high age (>75y , %)
- 2.5 - 3.5
- >3.5 - 4.5
- >4.5 - 5.5
- >5.5 - 6.5
- >6.5 - 7.5

Munich: 8.2

single households (%)
- 56 - 60
- 61 - 64
- 65 - 68
- 69 - 72

Munich: 54

unemployed (%)
- 1.3
- >1.3 - 1.7
- >1.7 - 2.8
- >2.8 - 3.3
- >3.3 - 7.4

Munich: 3.9

single households 65+ (%)
- 10 - 12
- >12 - 14.5
- >14.5 - 17
- >17 - 19.5
- >19.5 - 22

Munich: 23

Maxvorstadt: vulnerability indicators

state of data: 2015
data source: Indikatorenatlas München,
Landeshauptstadt München 2016

1 = Maßmannbergl
2 = Josephsplatz
3 = Am alten nördlichen
    Friedhof
4 = Universität
5 = Schönfeldvorstadt
6 = St. Benno
7 = Marsfeld
8 = Augustenstraße
9 = Königsplatz

0   0.75 1.5   3   4.5
Kilometers

N

Figure 24: Spatial distribution of all nine socio-economic indicators with reference value for total Munich (source: LH München, 2016)

40

4.2.4 Identification of high risk areas and position of critical infrastructure

Table 4 provides an overview of all risk indicators, including their means, standard deviation and pearson correlations. Significant correlations are marked with bold letters.

Table 4: Mean, standard deviation and pearson correlation for all indicators. Signficant correlations are marked in bold (p<0.01=**, p<0.5=*)

	foreigner (%)	unemployed (%)	65 years+ (%)	75 years+ (%)	<3 years (%)	single hh 65 (%)	single hh (%)	fluctuation (per 1000EW)	density (EW/m²)	trees (%)	distance (m)	Tmrt 2 pm (°C)
mean	29.2	3.1	12.1	5.3	2.6	15.2	67	392	1395	20.8	203	68
sd	9.5	1.7	2.9	1.5	0.6	3.8	4.8	63.3	1016	6.9	79	2.7
foreigner	1											
unemployed	**0.67***	1										
65years+	-0.45	0.19	1									
75years+	-0.62	-0.03	**0.95****	1								
<3 years	0.08	-0.5	-0.57	-0.43	1							
single hh 65	-0.27	0.03	**0.82****	**0.81****	-0.26	1						
single hh	-0.53	-0.07	0.43	0.38	-0.65	0.11	1					
fluctuation	0.08	-0.49	**-0.76***	-0.66	0.24	-0.61	-0.11	1				
density	-0.47	-0.24	-0.04	0.02	-0.04	-0.42	0.6	0.06	1			
trees	-0.35	-0.11	**0.67***	**0.76***	0.03	0.64	-0.14	-0.51	-0.11	1		
distance	-0.14	0.05	-0.2	-0.26	-0.19	**-0.68***	0.51	0.13	**0.8****	-0.11	1	
Tmrt 2 pm	0.46	0.16	-0.6	**-0.68***	0.01	-0.41	-0.24	0.48	-0.41	**-0.83****	-0.11	1

Unsurprisingly, strong positive correlations are observed for elderly living alone, high age and very high age. Furthermore there is a moderate positive correlation between percentage of foreigners and unemployed on 5% significance level. The data further suggest that city districts with a high percentage of older people experience less relocations, while very high age is positively correlated to vegetation amount. Since there exists an negative association between Tmrt at 2pm and tree amount, being 75 years or older is also negatively correlated with Tmrt at 2pm. Interestingly, elderly living alone are positively coupled with tree amount as well as negatively with distance to parks, while the data suggest no interdependency between these two. However, there is a strong positive relation between distance to green areas and population density, but

none between population density and tree amount. As parks smaller than 0.5ha were excluded from the density analysis, this finding probably indicates a lack of larger green spaces in denser populated neighbourhoods.

Aggregating all 11 vulnerability indicators, Am alten nördlichen Friedhof still has the highest level of vulnerability, followed by Josephsplatz and Augustenstraße. Different than with socio-economic indicators only, Marsfeld and Schönfeldvorstadt represent the least vulnerable district parts (see figure 25). The hazard map has been discussed in section 4.2.1. Combining the vulnerability and hazard assessment results in the final risk map (figure 25).

Relative to Maxvorstadt, Augustenstraße and Josephsplatz are at highest heat risk. Both have high vulnerability, but also high hazard scores. Josephsplatz is the densiest and also one of the least vegetated city district parts of Maxvorstadt. Its building structure is very homogenous and dominated by perimeter development with little to more densely vegetated inner courtyards. Similar to Augustenstraße, parks or larger open areas are absent. Augustenstraße has the highest percentage of single households and the highest fluctuation rate: Nearly 500 of 1000 inhabitants changed their residence, a niveau which has been constantly present since 2000 (LH München, 2016). Many bars and restaurants are located in Augstenstraße as well as Munich's popular theatre, grammar school Luisengymnasium and higher vocational school Städtische Berufsoberschule. Average distance to green is relatively high for Maxvorstadt (268m), the nearest park for Augustenstraße southern part is the old botanic garden and for the northern part Maßmannpark.

Königsplatz, Maxvorstadt's third largest CDP, is at high heat risk due to both high vulnerability and hazard scores. It has an exceptionally high percentage of unemployed and high shares of old people, yet constitutes also the least populated CDP of Maxvorstadt. For comparison, population density for Josephsplatz and Am alten nördlichen Friedhof is 30767 and 25586 EW/km² respectively whereas it is 1187 EW/km² for Königsplatz. However, Königsplatz is of high relevance since a majority of Maxvorstadt's museums are concentrated there and as it hosts the Technical University of Munich and borders Munich central main station in the south, large numbers of people spend their time in the city district part.
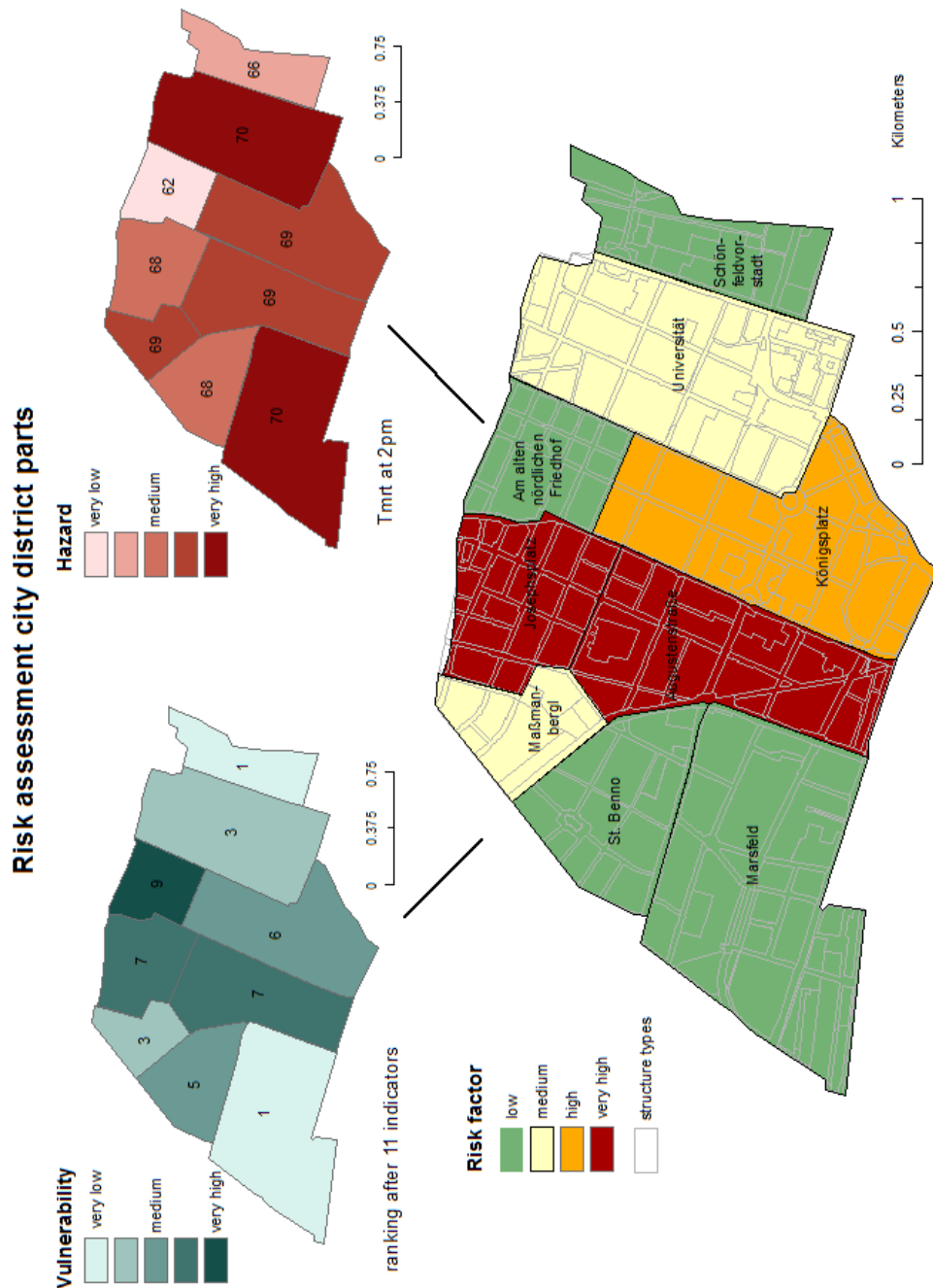
Figure 25: Vulnerability, hazard and risk map. Categories low –very high are assigned according to percentiles of the risk index: <50%=low, 50-75% medium, >75-95% high, >95% very high

The lowest heat risk was assessed for CDPs Am alten nördlichen Friedhof and Schönfeldvorstadt. While vulnerability as well as hazard level is low for Schönfeldvorstadt, Am alten nördlichen Friedhof unifies two extremes: The district part has the highest vulnerability as well as the lowest hazard level of Maxvorstadt. High population density and relatively high amounts of old and very old population are the main causes for the district part's increased vulnerability. On the other hand, Tmrt at 2pm is exceptionally low due to the large and densely tree covered green space "Alter nördlicher Friedhof". During this heat hour, the CDP is on average 4°C cooler than

the second coolest one. Since its vulnerability score is relatively close to the others, Am alten nördlichen Friedhof has on overall low risk level. As regards Marsfeld, a very high hazard level is outweighed by the very low vulnerability score: Due to the development area in the south, Marsfeld is Maxvorstadt's youngest city district part with the least amount of single households.

Retirement homes, hospitals, nurseries, kindergardens and schools have been defined as vulnerable social infrastructure. Figure 26 depicts the location of these institutions in combination with a fine scaled hazard map. Emergency service and medical center in Elisenstraße, medical center open med (Schleißheimer Straße), and private clinic Josephinum (Schönfeldstraße) were mapped as important medical infrastructure. Educational institutions comprise four elementary schools, two grammar schools as well as several higher vocational schools. Three retirement homes are located in Maxvorstadt: retirement homes Caritas (Hirtenstraße), Alten- und Servicezentrum Gabelsbergerstraße and retirement and foster home Hessstraße. Since no official list of all child caring institutions exists, adresses of kindergarden and nurseries were researched through internet inquiry. The resulting list of 59 institutions of municipal, free and private providers is probably not exhaustive, but the most complete listing available.

Most child caring institutions are located in the north of Maxvorstadt, where also population densities are highest (St. Benno, Josephsplatz, Am alten nördlichen Friedhof). An especially high concentration is visible in the east of St. Benno and in the proximity of the green space "Alter nördlicher Friedhof". While the medical center in Elisenstraße borders the "old botanic garden" and private clinic Josephinum benefits from the proximity to the "Englischer Garten", distance to green space is higher for medical center open med.
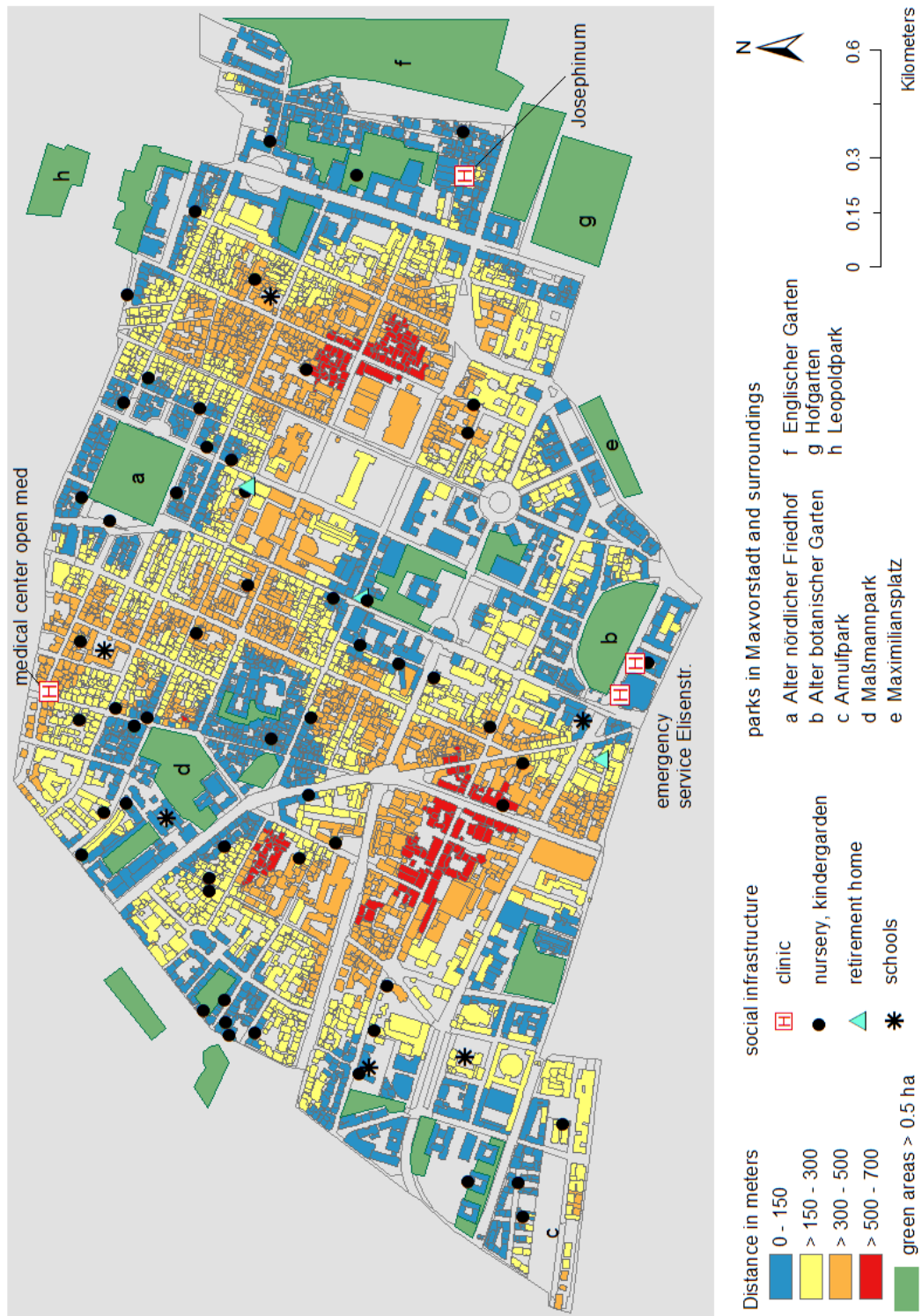
Figure 26:Map of walking distances to green areas greater than 0.5 ha and social infrastructure

5 Discussion

5.1 Hazard assessment

5.1.1 Tmrt development over time

A 2 m resolution was found to yield reasonable modelling results in acceptable computation time. The modeling day was selected after DWD criteria for heat days and tropical nights from the available time period 2000-2006. The measuring stations position in the research area constitutes a major advantage since disruptions from different environmental framework conditions are avoided. The T_{mrt} course of the selected modeling day (July 25th 2006) peaks at 2 pm and has its lowest point at 5 am in the morning. Considering the input data, it is shown that global radiation is a highly influential factor: While no radiation is measured before 6 am and after 9 pm, the highest radiation value (849.1W/m²) is recorded for 2 pm. For comparison, 3 and 4 pm were the hours with the highest air temperatures (33°C) and 6 am with the lowest (20.7°C). However, without radiation, the influence of T_{air} increases: Elevated nocturnal T_{mrt} values can be related to emitted longwave radiation as well as to relatively high air temperatures during the night. 5 am in the morning is the point in time with no incoming global radiation and low T_{air}, which is why it constitutes the T_{mrt} low. Pearson correlation analysis reveals a strong relationship for hourly mean T_{mrt} and T_{air} (r = 0.868**), but even stronger for hourly mean T_{mrt} and global radiation (r = 0.927**). Nevertheless, hourly maximum T_{mrt} values and global radiation are nearly perfectly correlated (r = 0.979**). Two additional days with different meteorological parameters, a randomly selected spring day (24th April 2006) and another summer heat day (21st July 2006), underline the importance of T_{air} and global radiation: Abrupt alterations in global radiation e.g. due to cloud formation are directly reflected by varying T_{mrt} values (see figure x). Though maximum radiation of 24th April is as high as of 21st July, moderate air temperatures (T_{max} 21.1°C, T_{mean} 15°C) lead to relatively high, but significantly lower T_{mrt} values than for the 21st July.

Lindberg et al. (2016a) and Onomura et al. (2015) confirm the large effect of T_{air} and global radiation on T_{mrt} under sunny and clear conditions, while Thorsson et al. (2014) also highlight that elevated T_{mrt} values can occur at rather low T_{air} if combined with high global radiation and relatively low diffuse radiation as was the case for 24th April 2006.
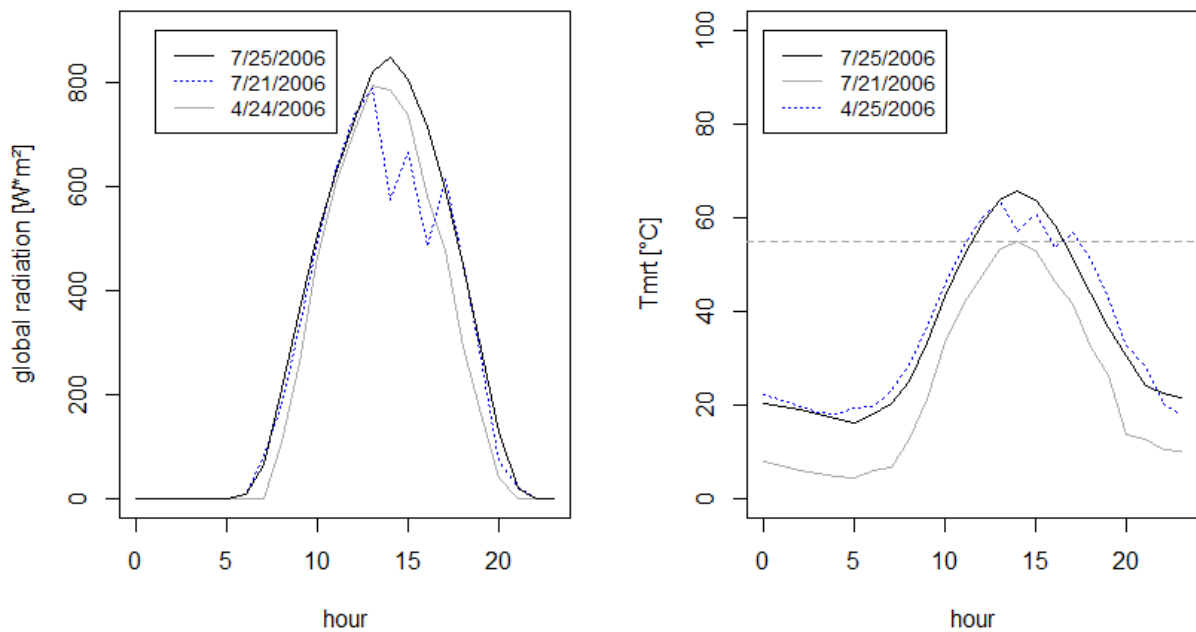
Figure 27: Global radiation and T_{mrt} over 24hrs for one spring and two summer days

5.1.2 Spatial patterns of T_{mrt}: influence of vegetation and urban parameters

Regarding the spatial patterns of T_{mrt} distribution, the largest variances between different sites are apparent during hours with elevated T_{mrt}. The highest variation is registered during 2-3 pm, the hour with the highest heat stress, while T_{mrt} distribution is most uniform during 6 am – 7 am in the morning and 7 to 9 pm in the evening.

Two main causes are responsible for this behavior: Firstly, with increasing T_{air} and global radiation the divide between sunlit and shaded sites becomes greater. Sunlit areas receive increasing amounts of incoming shortwave radiation, whereas shaded places are mainly governed by T_{air}. This also explains the sharp divide between very hot and cool sites and the nearly total absence of areas falling between these extremes. The coolest places during daytime are found in the shade of buildings or vegetation: Depending on the sun's position, these places shift over the course of a day: From morning until midday, the west-side of buildings is shaded, while it is the north side in the early afternoon and the east side in the evening. Open spaces with a high SVF represent the hottest areas during daytime. Thorsson et al. (2014) underline the importance of shadow patterns generated by obstructing objects such as trees, buildings and topography on T_{mrt} variations, but also point towards differences in thermal and radiative properties of the surrounding surface materials, i.e., albedo, emissivity, and heat capacity. However these are not considered in the current SOLWEIG model and thus didn't contribute to T_{mrt} variances. Investigating spatial distribution of T_{mrt} in London, Chatzipoulka et al. (2015) found that the radiant

environment can be predicted to great degree by urban geometry, such as height to width ratio of street canyons and street orientation. The analysis of Maxvorstadt showed that broad N-S running streets (e.g. Ludwigstraße) are warmer in the morning, but cooler during midday and the late afternoon than vast E-W oriented streets (e.g. Nymphenburgerstraße), due to different skyviewfactors and varying exposition towards the sun. Since shaded sites exhibit lower T_{mrt}, regardless if the shade is provided by buildings or vegetation, minimum and maximum T_{mrt} values didn't differentiate much between the scenario without greenery and the original scenario. Yet, as additional shade is provided if trees and bushes are included and less areas experience heat stress, mean T_{mrt} values were on average 2°C lower in the original setting.

Secondly, during nighttime, spatial patterns of elevated T_{mrt} distribution are reversed: until 7 am and after 8 pm highly obstructed areas, e.g. parks with a dense tree cover, exihibit warmer temperatures than open spaces. Comparison of T_{mrt} for an open space and a densely tree covered park revealed that the former was on average 10°C T_{mrt} cooler during nighttime, while it was on average 40°C warmer during midday and early afternoon (11am to 4pm). This reversed pattern is approved by a number of others studies on T_{mrt} (Coutts et al., 2016; Huang et al., 2008; Jänicke et al., 2015). While incoming shortwave radiation and outgoing longwave radiation fluxes are increased for open spaces, emission of shortwave and longwave radiation is restricted by trees (Fenner et al., 2014). Since emission of radiation is hampered by tree canopies, the cooling process is slowed down (Coutts et al., 2016; Wang and Akbari, 2016). Consequently, in the scenario without greenery and thus also increased skyviewfactors due to removal of obstructing objects, Maxvorstadt heats up more quickly and cools downs faster than in the original scenario with vegetation. However the cooling impact by trees during daytime largely outweighs slightly elevated temperatures during nighttime. With 20% increase in vegetation, the area exposed to severe heat stress during 2-3 pm was reduced from 75 to 58%, while nocturnal temperatures were well below the heat stress threshold. Due to nocturnal radiation trapping and the large influence of shadow patterns during daytime, T_{mrt} variances are lowest during the transition between day and nighttime and highest during hours with maximums of global radiation and air temperature.

Lindberg et al. (2016) explored the impact of building density and vegetation cover on Tmrt for a case study site in Stockholm, Sweden using SOLWEIG. Similarly, highest Tmrt occured in open and generally sunlit locations. Dense urban structures were found to effectively reduce outdoor heat stress due to self-shading of buildings and reduced skyviewfactors. Overall, an almost linear decrease of T_{mrt} with increasing vegetation cover was observed, while additional vegetation had more effect in the low building density than in dense urban setting. With low buildings density, no-vegetation and conventional (3% tree cover) vegetation proposals show much larger differences in T_{mrt} than conventional and abundant (8.6% tree cover) proposals.

Exploring the relationship between vegetation coverage and T_{mrt} at 2 pm, large deviations for sites with high (over 80%) vegetation amount where revealed. Differences between these structure units amounted to as much as 44°C T_{mrt}. After exclusion of these sites, a linear trend became observable. These deviations can be explained by the fact that high vegetation amount does not specify whether the area is covered by grass, bushes or trees. As land cover is not considered in SOLWEIG, lawns are treated equally as asphalt covered surfaces. However not taking into account grass areas was not seen as a major deficit since the main effect of vegetation in reducing hot temperatures is through shading (Mayer, 1993). Studying the spatial distribution of T_{mrt} in Berlin, Jänicke et al. (2015) even excluded vegetation below 2m as it was suggested to have only a minor effect on shading. Furthermore, cooling by evapotranspiration depends largely on the condition of vegetation: Scarcity of water which is likely to occur during a heatwave significantly inhibits the cooling capacity (Coutts et al., 2016; Gill, 2006; Lindberg et al., 2016a). Due to its shallow rooting depth, grass is likely to be the first type of vegetation to suffer poor water availability, curtailing the effect of evapotranspiration (Gill, 2006). Thus, Potchter et al. (2006) found that urban green space covered entirely by grass can be warmer than surrounding areas under drought conditions. Validating SOLWEIG's new ground cover schemes which allows to define thermal and radiative properties for certain surfaces (e.g. grass, dark and light asphalt), (Lindberg et al., 2016a) found that ground cover classes had only little effect on T_{mrt} compared to T_{air} and shading. Erell et al. (2014) report that increasing the albedo of urban surfaces, leading to a reduction in longwave radiation fluxes is likely to be counterbalanced by increased reflection of shortwave radiation. Despite this minor effect on the outdoor environment, ground cover types and surface materials play a decisive role for indoor building temperatures and should be considered if assessing indoor thermal comfort.

5.1.3 Limitation and uncertainties

Due to its high variability compared to air temperature (Ali-Toudert and Mayer, 2006; Lindberg et al., 2016) and dominating influence on PET on clear and sunny days (Matzarakis et al., 2010), T_{mrt} is regarded as a good predictor for heat stress and mortality (Mayer, 1993; Thorsson et al., 2014). Nevertheless it should be kept in mind that wind speed and relative humidity, which constitute important parameters for human thermal comfort, are not or only marginally considered.

ENVI-met and Rayman are alternative models for assessing T_{mrt}. Being the most elaborate and more complex program than SOLWEIG, ENVI-met has high computational demands and is thus best for smaller local simulations. While Rayman only produces results for one point (Matzarakis et al., 2010), Solweig is able to simulate T_{mrt} for large areas with high spatial resolution (Lindberg and Grimmond, 2011a; Jänicke et al., 2015). In several studies using a bigger research scope, SOLWEIG simulated T_{mrt} closest to the observation (Chen et al., 2014; Jänicke et al., 2015).

In SOLWEIG, relative humidity is used for estimating the emissivity of the sky to simulate incoming long-wave radiation and to calculate direct and diffuse radiation from global radiation if these measures are not available (Lindberg and Grimmond, 2011). However, Onomura et al. (2015) assessed little sensitivity of simulated Tmrt in SOLWEIG towards relative humidity. If direct and diffuse radiation data are not available, SOLWEIG offers to calculate these parameters using the approach by Reindl (1990) (Lindberg and Grimmond, 2011). Since these data are often not available, this constitutes a handy possibility. Yet, comparison of model runs with calculated and measured radiation data (for the second run, direct radiation was determined by substracting diffuse from global radiation) showed considerable differences in T_{mrt} outcomes, as fractions of diffuse and direct radiation varied. Jänicke et al. (2015) confirm a high sensitivity of T_{mrt} in SOLWEIG to direct or diffuse radiation.

Since the selected meteorological data had an hourly resolution, T_{mrt} was analysed on an hourly basis. With these settings, SOLWEIG generates shadow patterns in the middle of each hour, thus if a place changes from a shaded to a sunlit position within this hour, this change is not considered (Lindberg and Grimmond, 2011). Consequently, T_{mrt} is slightly over- or underestimated. Yu et al. (2009) suggest a 10 min resolution to correctly assess shadow patterns for complex urban patterns. Weighting up the distinct increase in computational time against minor improvements in T_{mrt} calculation, an hourly resolution was found to be reasonable for this research scope.

Two options for implementing vegetation in SOLWEIG exist: A vegetation DSM can either be created from a text file providing information about xy-position, diameter, height and trunk height or gridded vegetation data can be directly used as an input which needs to be differentiated in a trunk and canopy zone layer. Per default, the trunk zone layer is created from canopy layer as 0.25 percent fraction. This option was also selected for this analysis, yet real conditions are likely to deviate. Furthermore, SOLWEIG does not distinguish between coniferous and deciduous trees or different tree species. For instance, small leafed species have a different cooling impact than larger leafed ones (Doick et al., 2013). Nevertheless, the shade provided by the crown is realistically assessed since gridded vegetation data is demanded as modelling input.

Neither wind fields nor variations in building wall materials are considered in the current version of the model (Solweig 2015a) (Lindberg et al., 2016b). A newly developed ground cover scheme allows to alter albedo and heat emissitivity for different ground covers such as grass, water and dark asphalt. Since no detailed ground cover data were available and due to Lindberg et al. (2016b) finding that it had only minor influence on T_{mrt} ground surfaces (maximum of 5°C variance compared to the original model) were not distinguished in this analysis. Ground albedo

and emissivity were left to the default values of 0.2 and 0.95 respectively. However, for refined modeling results, surface characteristics should be considered as additional modeling input. The importance of this parameter is likely to increase with a research design that aims to analyse differences between outer and inner city district parts with varying degrees of built up or natural structures or a site specific assessment that explores different planning scenarios.

To reduce computational time, resolution size was reduced to 2m x 2m. Despite a good overall fit, young trees or single trees with a small treetop thus might be peculated. For example, Arnulfpark in south of city district part Marsfeld exhibited one of the highest heat loads during 2-3 pm, although the park has a high vegetation cover and several single tree plantings. However the park was only established in 2004 and is largely dominated by grass areas. Trees are planted rather sparsely and haven't yet developed mature crowns. Thus, T_{mrt} is likely to be slightly overestimated, but the cooling effect of the vegetation in Arnulfpark has to be considered as low.

In order to value the human thermal comfort, temperatures above 55.5°C T_{mrt} were defined as heat stress situations according to Thorsson et al. (2014). Above that threshold, the number of death among elderly increased significantly. It has to be acknowledged that this heat-mortality relationship was assessed for Goteborg in the south of Sweden, which has different climatic conditions than Munich. Since people adapt to the local climate (Gosling et al., 2009; Loughnan et al., 2013), a different threshold might be more appropriate for Munich. Though several heat stress analysis were carried out for different regions in Germany (e.g. Gabriel and Endlicher, 2011; Ketterer and Matzarakis, 2014; Lissner et al., 2012), none defined an heat threshold in T_{mrt}, but rather in T_{air} or PET. Studying T_{mrt} distribution in Berlin and Shanghai, Jänicke et al. (2015) and Chen et al. (2016) also referred to the work of Thorsson and colleagues, which constitutes the only study so far that has analysed T_{mrt}-mortality relationships. Chen found that SOLWEIG overestimates T_{mrt} by 4°C.

However, T_{mrt} values for Maxvorstadt in sunlit spaces during midday and afternoon were well above the heat threshold, so heat stress sensation can be assumed despite these local differences. Beside this local component for human thermal comfort, it has to be acknowledged that individual heat stress sensations might differ largely due to age, clothing, activity and personal preferences (Gosling et al., 2009; Smoyer-Tomic et al., 2003). Thus, individuals might experience heat stress and negative health impacts even below these generalized heat thresholds.

Furthermore it has to be noted that this analysis estimated outdoor heat stress only. Yet, high nocturnal indoor temperatures are said to have an especially hazardous effect as there is no relief from the daily heat (Buchin et al., 2016; Loughnan et al., 2013). Integration of indoor building temperatures is therefore likely to improve heat risk assessments (Scherber et al.,

2014). Scherer et al. (2013) point to the fact that many of elderly people who have a raised vulnerability towards heat, are less mobile and remain inside the building the whole day. Thus, they might be less affected by outdoor than by indoor heat stress. Appropriate assessment of indoor building temperatures demands detailed information about building age, insulation and access to air conditioning (Buchin et al., 2014), data which are rarely availably for whole city districts or neighbourhoods.

5.2 Vulnerability and heat risk assessment

5.2.1 Evaluation of heat vulnerability indicators

While large consensus exist that vulnerability assessment is a helpful asset in determining heat risk and directing of planning priorities (e.g. Johnson et al., 2012; Wolf et al., 2011), its implementation is less agreed upon: Such, various heat vulnerability indexes have been developed during the last years (Bao et al., 2015; Romero-Lankao et al., 2012). Comparability between different studies is limited since considered indicators, weighting factors and aggregation method vary considerably (see section 2.2.2 and appendix 1). As regards this analysis, selection of indicators was based upon a list of most common heat vulnerability indicators, local characteristics and data availability. Thus, information about medical predisposition could not be included in the vulnerability index since these data were not available for Maxvorstadt. Prevalence of AC was not regarded as this factor is seen to have little influence in Germany compared to the US (Johnson et al., 2012). To maximize transparency and objectivity, introduction of further weighting factors and classifications was avoided: Such, all factors were weighted equally and no distinction was made among vulnerability indicators for exposure, adaptive capacity and sensitivity. In absence of absolute thresholds, indicators were standardized to allow for a comparison of relative vulnerability for the selected study site.

Different to other heat vulnerability indicators, tree instead of vegetation cover was incorporated as a factor for the physical environment. This is considered as an important improvement, as it was shown that T_{mrt} is stronger correlated with the percentage of trees than with the fraction of vegetation due to reasons discussed in the paragraphs above. Proximity to green urban areas was incorporated as second physical indicator. For assessing distances to green space, three major questions have to be answered (Koppen et al., 2014): Which areas are taken into consideration? For whom? How is distance measured? In this analysis, only green spaces with trees and a size greater than 0.5ha were considered, since the main interest was the provision of cool areas by urban green spaces. Neighbouring green spaces, such as Englischer Garten were included for full assessment. The buffer distance to include that neighbouring spaces was set to 300m according to the ANGST standards that define this distance as a 5min walking time (Natural England, 2009). However, walking times differ among different age groups and mobility levels: Koppen et al. (2014) suggest that little children and elderly need rather 10min to cover a

distance of 400m and thus will prefer shorter distances to neighbouring green spaces. Moreover, individual willingness to walk a certain distance to a park is influenced by personal perceptions of a park's quality and characteristics of the walking route: Whereas a positively received park may attract visitors from farther distances (Moseley et al., 2013), a shadowy park nearby might be avoided due to noise impact or feelings of unsafety. While Sarkar et al. (2015) found that streets lined with trees provide an incentive to walk due to positive associations with street environmental quality, larger height differences or the need to cross major traffic roads obtain the opposite effect. Observations of real park usage and interviews with residents are able to uncover behavioural patterns, yet these could not be considered in the scope of this study.

Buffer and network analysis represent the most common approaches to measures distances (Koppen et al., 2014). For this analysis, proximity to urban green space was assessed using cost distance analysis instead, where the selected green spaces were defined as "sources" and buildings as "barriers" to realistically calculate walking distances. Buffer analysis only computes linear distances and neglects obstacles that pedestrians have to circumvent. Thus, when also considering green spaces below 0.5ha, average distance is 49.5m for buffer and but quadrupled (209m) for cost distance analysis. Network analysis has higher computational demands and is more time-consuming to perform since junctions, edges and connecting rules have to be defined. Moreover, it constrains pedestrians to streets and paths, while shortest crossing of open spaces is possible in cost distance analysis. The chosen approach also acknowledges access limitations: Since buildings represent barriers, only adjacent houses have access to inner courtyard green spaces while public parks are usually not completely enclosed with buildings. However the location of park entrances and house exits are not regarded and modification of e.g. walking speeds like in network analysis is not possible.

Similar to other prominent indexes (Harlan et al., 2006; Johnson et al., 2012; Reid et al., 2009), three factors in the current approach address old age (percentage inhabitants being more than 64 years and 74 years old, fraction of single househoulds older than 64). As these indicators are highly correlated with each other (see section 4.2.4), city district parts with a relatively high number of old people, e.g. "Am alten nördlichen Friedhof" were assigned with a high vulnerability score three times, whereas high percentage of unemployment (CDP Königsplatz) and high fluctuation (CDP Marsfeld, Augustenstraße) was only regarded once. Thus, the parameter "old age" might be overrepresented in the index. If age is only considered once, CDP Am alten nördlichen Friedhof is overtaken by Josephsplatz and Augustenstraße as the most vulnerable CDP. Otherwise positions in the vulnerability ranking don't differ much which suggests that apart from Am alten nördlichen Friedhof, vulnerability or resilience of individual CDPs is rather reducible to multiple factors and not to a single cause.

5.2.2 Planning implications for Maxvorstadt

For mitigation towards heat by urban planning, two measures have a significant impact on shadow patterns and thus on Tmrt: Densification of building structure (Ketterer and Matzarakis, 2014; Lindberg et al., 2016b) and expanding of vegetation cover. While air quality and ventilation might be negatively affected in narrow streets and dense urban fabrics, vegetation stores and reradiates less heat than built surfaces and provides additional benefits such as carbon sequestration and air purification (Gago et al., 2013; Gill et al., 2007; McPherson et al., 1994).

As has been already discussed in section 2.3, the cooling effect of urban green is largely dependent on size, type of vegetation and location. Tree plantings are most effective in open spaces and wide street canyons with N-S orientation, since these places exhibit the highest heat stress during the maximum heat hours. Priority street canyons for street trees can be identified employing the method of Norton and colleagues (2015), where street canyons in vulnerable neighbourhoods are ranked according to their geometry and orientation. Wide roads with high solar exposure and lack of shade from vegetation are accorded top priority. Applied to Maxvorstadt, Augustenstraße was one of the CDPs with the highest heat risk. Analysing shadow patterns and vegetation cover (see appendix x), need for action is identified for the north side of main road Marsstraße running from E to W and N-S oriented street Augustenstraße. Unlike its northern part, the southern segment between Karlstraße until Briennerstraße is unvegetated. Additional street trees in these locations will provide shade for pedestrians and adjacent buildings, increasing human thermal comfort and energy savings. However, to allow wind flow and prevent trapping of congestions, treetops should not form a continuous canopy (Spronken-Smith and Oke, 1999). Trees planted in proximity to buildings can potentially cause damage to the foundation level of the houses due to changes in soil moisture (Gill et al., 2007). Thus, respective plantings should be discussed with affected residents and store owners to detect possible usage conflicts and concerns (usage as parking lot or outdoor area of bars).

As regards open spaces, high tree cover reduces T_{mrt} loads, yet a mixture of bushes, small meadows and trees is likely to be the better design solution. Firstly, shaded areas cause thermal discomfort in seasons with low air temperatures, when sunlit areas with incoming shortwave radiation are preferred. Deciduous trees provide shade in summer and allow more solar radiation to penetrate in winter than evergreen trees (Lindberg et al., 2016). Secondly, since individual perceptions of thermal comfort differ, a range of different microclimatic conditions as offered by a mixed vegetation structure is likely to satisfy more people (Katzschner, Lutz et al., 2007; Matzarakis and Mayer, 2000). Such, interviewed pedestrians in Dresden were very tolerant towards heat stress as long as they could choose between different microclimatic settings (Katzschner, 2010). Consequently, e.g. tree cover of Arnulfpark in CDP Marsfeld should not be increased to 90%, but densification of single tree spots would provide cool islands in the largely grass dominated park.

Additional irrigation during dry, hot summers can help to maximize cooling benefits from existing UGI (Norton et al., 2015). During extreme heat, urban trees have an extraordinary water use (Coutts et al., 2016), while at the same time water supplies might be low. In order to avoid this conflict, Gill et al. (2007) suggest measures such as rainwater harvesting, re-use of greywater and floodwater storage. Moreover, several tree species from temperate zones that need less water supply and are less sensible towards droughts could be an alternative (Gill et al., 2007). Overall, plantings and maintenance of street trees (including expenditure for damage removal) are costly, however McPherson et al. (2016) found that the monetized value of annual services from California's street trees largely outweighs their costs: Average annual tree management cost of $19 per tree opposed $111 annual value of services per tree (McPherson et al., 2016).

High population density was strongly correlated with increased distance to shaded green spaces. While dense building structures and narrow streets hinder implementation of larger UGI, green facades and green walls constitute possible physical adaptation strategies.

In neighbourhoods with high socio-economic vulnerability or little capacities to enhance green space possible adaptation measures include implementation of social support systems for vulnerable individuals, such as neighbourhood buddy systems (Chuang, 2013) or heat hotlines, where people can call for help or advise during extreme heat events (Uejio et al., 2011). Designation of air-conditioned cooling centers (e.g. in libraries, museums, senior centers) where people can recover from extreme heat (Chuang, 2013) provides both support for residents and people in outdoor places. Today, cooling centers are solely found in US cities (e.g. New York, Chicago, Phoenix), but under the impression of current climate change could also constitute a possible strategy for European urban areas.

5.2.3   Limitations and future directions

Elevated temperatures do not only affect Maxvorstadt residents, but also tourists and workers that spend their day there. Maxvorstadt has an especially high number of daytime visitors, up to four times more people than actually live there. Though Marsfeld, Königsplatz have relatively low population densities, the number of affected people is considerably higher. Moreover, socio-economic characteristics of these daytime visitors and thus their vulnerability level can't be directly assessed. Due to this reason, the mapping of retirement homes, child caring institutions, schools and hospitals is relevant as it provides valuable information about concentration of vulnerable people. As regards tourists, socio-economic characteristics and respective vulnerability are less deducible. Contrary to other groups however, their stay in a certain place is voluntary and they have more options to avoid heat stress and relocate themselves in cooler places.

It has to be stressed that the presented approach is suitable to identify areas of priority within a certain region but does not allow to draw general conclusions about an area's heat risk. Since no findings exist which amount of e.g. elderly is to be regarded as critical as it significantly increases vulnerability, indicator values could not be classified according to a fixe scale, but rather were compared to find relative thresholds. Such, classification of high and low vulnerability or heat risk are highly depending on the chosen research scope. Seen in relation to Munich, CDP Augustenstraße might be even assessed a low risk level if conditions in other city district parts are worse.

Due to the limited spatial resolution of publicly available socio-economic data for Maxvorstadt, risk assessment had to be restricted to city district part level. Block level analysis would have provided more specific information about heat risk hot spots. GIS analysis of physical environment indicators and T_{mrt} modeling depicted large differences within city district parts, which are not represented in the current risk index. In fact, parts of Josephsplatz or Augustenstraße might be less affected than parts of other city districts. However, since SOLWEIG is suitable to model T_{mrt} for extensive areas, the presented approach could be as well applied to a larger study area where it would yield informative results despite restrictions due to data privacy issues.

6   Conclusion

Elevated air temperatures are associated with negative impacts on human health, ranging from thermal discomfort to increased mortality numbers during heat events. Increasing frequency and magnitude of heat waves in the 21st century due to climate change pose a particular thread towards cities, exacerbating the urban heat island effect. Heat risk assessments play an important role for prevention of heath-related death and adaptation of cities to extreme heat events. So far, many heat risk studies either only modeled heat impacts without considering the populations vulnerability or developed vulnerability indexes, but didn't analyse spatial and temporal hazard distribution. The approach presented here combines spatially explicit hazard assessment with vulnerability analysis on neighbourhood-scale.

On clear and calm days, T_{mrt} is reported to be the most important meteorological parameter influencing human energy balance and heat load and thus governing human thermal comfort. The radiation flux model SOLWEIG, DEMs of buildings and vegetation as well as meteorological input data of heat day 25th July 2006 were used to model distribution of T_{mrt} patterns for study site Maxvorstadt over 24 hours. For the chosen modelling day, the highest T_{mrt} loads are observable between 2-3 pm, the lowest from 5-6 am. Global radiation and T_{air} are identified as the most important meteorological parameters influencing T_{mrt}. Shadowing by buildings and vegetation equally lowers T_{mrt} during daytime, while building height, street orientation and street width are decisive for the shading effect of buildings. Amount of trees rather than vegetation percentage shows a negative linear relationship with T_{mrt} during 2-3 pm (r= -0.73** compared to r=-0.63**): the higher the tree fraction, the lower T_{mrt} loads. Open, unobstructed spaces are hottest during daytime and coolest during nighttime, while the opposite applies to densely tree covered sites. Whereas minimum and maximum T_{mrt} for the former differ up to 70°C, it is only 20°C for the latter as dense tree canopies effectively reduce diurnal heat, but also hinder longwave radiation cooling during nighttime. However the diurnal cooling effect of trees outweighs slightly elevated nighttime temperatures: With Maxvorstadt's current planting scenario, the area under heat stress during 2-3 pm is reduced from 73% without any vegetation to 55%. Seen over 24 hours, mean T_{mrt} is 2°C lower with vegetation.

Increasing vegetation cover of perimeter buildings blocks by tree plantings has only little impact on reducing T_{mrt} since the dense building structure is likely to dominate shadow patterns. Additional shade from trees has only little effect. Anyhow, cooling through evapotranspiration by trees, grass, green facades or green walls was not considered in this study. As it constitutes the diurnal heat stress maximum, T_{mrt} during 2-3 pm was chosen for the heat risk index.

Nine socio-economic and two physical environment indicators (percentage of trees and proximity to parks) were selected for the vulnerability assessment. Tree coverage was preferred over vegetation coverage as an indicator since it is the most important vegetation type for heat mitigation and more strongly correlated with T_{mrt}. Though Maxvorstadt is generally a relatively young city district part with a high proportion of single households compared to the rest of Munich, variables differed considerably between Maxvorstadt's city district parts, underlining the importance of spatially specific vulnerability assessments.

In the case study of Maxvorstadt, accuracy of risk analysis was restricted by low spatial resolution of socio-economic data and lack of information about health conditions. Nevertheless, the case study showed the additional value if both hazard and vulnerability information are incorporated when assessing heat risk. If only T_{mrt} distributions had been considered, CDPs Marsfeld and Universität would have been identified as the regions with the highest heat risk, while combination of both assessments showed that CDPs Josephsplatz and Augustenstraße have a double burden of high heat hazard and high heat vulnerability demanding increased priority. The mapping of vulnerable social infrastructure can provide additional valuable information for identification of priority sites within high risk neighbourhoods.

The presented approach is able to assess outdoor heat stress, yet it should be noted that indoor temperatures might be more relevant for especially vulnerable groups such as sick or elderly people with limited mobility. Refinements for T_{mrt} modelling results – higher spatial and temporal resolution, exact instead of general trunk zone creation and implementation of ground cover scheme - have been discussed. While the first two are supposed to be of minor importance, consideration of ground cover characteristics which might be further improved in future SOLWEIG versions, could provide information for selection of urban materials and site design.

Further research should investigate the relationship between thermal comfort perceptions and T_{mrt} to provide an adapted heat threshold and comfort zones for Germany. This can be either done by interviews and on-site measurements or statistical analysis of mortality data and T_{mrt} observations.

Enhancing green infrastructure constitutes a favourable heat mitigation strategy, since it can be implemented in the existing building structure and provides supplementary benefits. Priority locations for trees are sun-exposed open spaces or wide N-S oriented street canyons. Specific measurements can be best identified by urban planners in dialogue with affected stakeholders. The presented approach provides spatially specific heat risk information and thus constitutes a valuable planning guidance.

7 References

Ali-Toudert, F., Mayer, H., 2006. Numerical study on the effects of aspect ratio and orientation of an urban street canyon on outdoor thermal comfort in hot and dry climate. Building and Environment 41, 94–108. doi:10.1016/j.buildenv.2005.01.013

Bao, J., Li, X., Yu, C., 2015. The Construction and Validation of the Heat Vulnerability Index, a Review. International Journal of Environmental Research and Public Health 12, 7220–7234. doi:10.3390/ijerph120707220

Benzie, M., 2012. Social Justice and Adaptation in the UK. Presented at the The Governance of Adaptation: An international symposium, Amsterdam, p. 23.

Bradford, K., Abrahams, L., Hegglin, M., Klima, K., 2015. A Heat Vulnerability Index and Adaptation Solutions for Pittsburgh, Pennsylvania. Environmental Science & Technology 49, 11303–11311. doi:10.1021/acs.est.5b03127

Brown, R.D., 2011. Ameliorating the effects of climate change: Modifying microclimates through design. Landscape and Urban Planning 100, 372–374. doi:10.1016/j.landurbplan.2011.01.010

Brown, S., Walker, G., 2008. Understanding heat wave vulnerability in nursing and residential homes. Building Research & Information 36, 363–372. doi:10.1080/09613210802076427

Buchholz, S., Kossmann, M., 2015. Research note. Visualisation of summer heat intensity for different settlement types and varying surface fraction partitioning. Landscape and Urban Planning 144, 59–64. doi:10.1016/j.landurbplan.2015.08.002

Buchin, O., Hoelscher, M.-T., Meier, F., Nehls, T., Ziegler, F., 2016. Evaluation of the health-risk reduction potential of countermeasures to urban heat islands. Energy and Buildings 114, 27–37. doi:10.1016/j.enbuild.2015.06.038

Buchin, O., Jänicke, B., Meier, F., Scherer, D., Ziegler, F., 2014. The role of building models in the evaluation of heat-related risks. Natural Hazards and Earth System Sciences Discussions 2, 7621–7650. doi:10.5194/nhessd-2-7621-2014

Carter, J.G., Cavan, G., Connelly, A., Guy, S., Handley, J., Kazmierczak, A., 2015. Climate change and the city: Building capacity for urban adaptation. Progress in Planning 95, 1–66. doi:10.1016/j.progress.2013.08.001

Chen, Y.-C., Lin, T.-P., Matzarakis, A., 2014. Comparison of mean radiant temperature from field experiment and modelling: a case study in Freiburg, Germany. Theoretical and Applied Climatology 118, 535–551. doi:10.1007/s00704-013-1081-z

Chow, W.T.L., Chuang, W.-C., Gober, P., 2012. Vulnerability to Extreme Heat in Metropolitan Phoenix: Spatial, Temporal, and Demographic Dimensions. The Professional Geographer 64, 286–302. doi:10.1080/00330124.2011.600225

Chuang, W.-C., 2013. Vulnerability to Heat Stress in Urban Areas: A Sustainability Perspective. Arizona State University.

Chuang, W.-C., Gober, P., 2015. Predicting Hospitalization for Heat-Related Illness at the Census Tract Level: Accuracy of a Generic Heat Vulnerability Index in Phoenix, Arizona (USA). Environmental Health Perspectives. doi:10.1289/ehp.1307868

Coutts, A.M., White, E.C., Tapper, N.J., Beringer, J., Livesley, S.J., 2016. Temperature and human thermal comfort effects of street trees across three contrasting street canyon environments. Theoretical and Applied Climatology 124, 55–68. doi:10.1007/s00704-015-1409-y

Depietri, Y., Welle, T., Renaud, F.G., 2013. Social vulnerability assessment of the Cologne urban area (Germany) to heat waves: links to ecosystem services. International Journal of Disaster Risk Reduction 6, 98–117. doi:10.1016/j.ijdrr.2013.10.001

Deutscher Wetterdienst (DWD), 2016a. Meteorologische Kenntage. Available from: https://www.dwd.de/DE/service/lexikon/Functions/glossar.html?lv2=101334&lv3=101452. Last accessed: 6/7/2016.

Deutscher Wetterdienst (DWD), 2016b. Hitze- und UV-Warnungen. Available from: http://www.dwd.de/DE/wetter/warnungen_aktuell/kriterien/uv_hitze_warnungen.html. Last accessed: 6/7/2016.

Doick, K.J., Hutchings, T., Great Britain, Forest Research, Great Britain, Forestry Commission, 2013. Air temperature regulation by urban trees and green infrastructure. Forestry Commission, Farnham, Surrey.

Dugord, P.-A., Lauf, S., Schuster, C., Kleinschmit, B., 2014. Land use patterns, temperature distribution, and potential heat stress risk – The case study Berlin, Germany. Computers, Environment and Urban Systems 48, 86–98. doi:10.1016/j.compenvurbsys.2014.07.005

Feyisa, G.L., Dons, K., Meilby, H., 2014. Efficiency of parks in mitigating urban heat island effect: An example from Addis Ababa. Landscape and Urban Planning 123, 87–95. doi:10.1016/j.landurbplan.2013.12.008

Fryd, O., 2011. The role of urban green space and trees in relation to climate change. CAB Reviews: Perspectives in Agriculture, Veterinary Science, Nutrition and Natural Resources 6. doi:10.1079/PAVSNNR20116053

Gabriel, K.M.A., Endlicher, W.R., 2011. Urban and rural mortality rates during heat waves in Berlin and Brandenburg, Germany. Environmental Pollution 159, 2044–2050. doi:10.1016/j.envpol.2011.01.016

Gago, E.J., Roldan, J., Pacheco-Torres, R., Ordóñez, J., 2013. The city and urban heat islands: A review of strategies to mitigate adverse effects. Renewable and Sustainable Energy Reviews 25, 749–758. doi:10.1016/j.rser.2013.05.057

Gill, S.E., 2006. Climate Change and Urban Greenspace. University of Manchester, UK.

Gill, S.E., Handley, J.F., Ennos, A.R., Pauleit, S., 2007. Adapting cities for climate change: the role of the green infrastructure. Built environment 33, 115–133.

Gosling, S.N., Lowe, J.A., McGregor, G.R., Pelling, M., Malamud, B.D., 2009. Associations between elevated atmospheric temperature and human mortality: a critical review of the literature. Climatic Change 92, 299–341. doi:10.1007/s10584-008-9441-x

Harlan, S.L., Brazel, A.J., Prashad, L., Stefanov, W.L., Larsen, L., 2006. Neighborhood microclimates and vulnerability to heat stress. Social Science & Medicine 63, 2847–2863. doi:10.1016/j.socscimed.2006.07.030

Herrmann, J., Matzarakis, A., 2012. Mean radiant temperature in idealised urban canyons—examples from Freiburg, Germany. International Journal of Biometeorology 56, 199–203. doi:10.1007/s00484-010-0394-1

Hondula, D.M., Davis, R.E., Leisten, M.J., Saha, M.V., Veazey, L.M., Wegner, C.R., 2012. Fine-scale spatial variability of heat-related mortality in Philadelphia County, USA, from 1983-2008: a case-series analysis. Environmental Health 11. doi:10.1186/1476-069X-11-16

Huang, L., Li, J., Zhao, D., Zhu, J., 2008. A fieldwork study on the diurnal changes of urban microclimate in four types of ground cover and urban heat island of Nanjing, China. Building and Environment 43, 7–17. doi:10.1016/j.buildenv.2006.11.025

IPCC, 2007. *Climate Change 2007: Impacts, Adaptation and Vulnerability. Contribution of Working Group II to the Fourth Assessment Report of the Intergovernmental Panel on Climate Change,* M.L. Parry, O.F. Canziani, J.P. Palutikof, P.J. van der Linden and C.E. Hanson, Eds., Cambridge University Press, Cambridge, UK.

IPCC, 2012. Managing the Risks of Extreme Events and Disasters to Advance Climate Change Adaptation. A Special Report of Working Groups I and II of the Intergovern-mental Panel on Climate Change Field, C.B., V. Barros, T.F. Stocker, D. Qin, D.J. Dokken, K.L. Ebi, M.D. Mastrandrea, K.J. Mach, G.-K. Plattner, S.K. Allen,M. Tignor, and P.M. Midgley (eds.). Cambridge University Press, Cambridge, UK, and New York, NY, USA.

Jänicke, B., Meier, F., Lindberg, F., Schubert, S., Scherer, D., 2015. Towards city-wide, building-resolving analysis of mean radiant temperature. Urban Climate 15, 83–98. doi:10.1016/j.uclim.2015.11.003

Jauregui, E., 1990. Influence of a large urban park on temperature and convective precipitation in a tropical city. Energy and Buildings 15, 457–463. doi:10.1016/0378-7788(90)90021-A

Johnson, D.P., Stanforth, A., Lulla, V., Luber, G., 2012. Developing an applied extreme heat vulnerability index utilizing socioeconomic and environmental data. Applied Geography 35, 23–31. doi:10.1016/j.apgeog.2012.04.006

Kalkstein, L.S., Sheridan, S.C., Kalkstein, A.J., 2009. Heat/health warning systems: development, implementation, and intervention activities, in: Biometeorology for Adaptation to Climate Variability and Change. Springer, pp. 33–48.

Katzschner, Lutz, Mayer, Helmut, Drey, C., Bruse, M., 2007. Strategies and concepts for thermal comfort discussions in urban planning to mitigate the impacts of climate extremes. Presented at the PLEA2007-The 24th Converence on Passive and Low Energy Architecture, Singapore, p. 6.

Katzschner, L., 2011. Urban Climate Strategies Against Future Heat Stress Conditions. – In: Zimmerman, O., 2011. Resilient cities: cities and adaptation to climate change - pro-ceedings of the Global Forum 2010, Local sustainability. Springer, Dordrecht, pp. 79-89.

Ketterer, C., Matzarakis, A., 2014. Human-biometeorological assessment of heat stress reduction by replanning measures in Stuttgart, Germany. Landscape and Urban Planning 122, 78–88. doi:10.1016/j.landurbplan.2013.11.003

Koppen, G., Sang, Å.O., Tveit, M.S., 2014. Managing the potential for outdoor recreation: Adequate mapping and measuring of accessibility to urban recreational landscapes. Urban Forestry & Urban Greening 13, 71–83. doi:10.1016/j.ufug.2013.11.005

Krüger, E., Drach, P., Emmanuel, R., Corbella, O., 2013. Assessment of daytime outdoor comfort levels in and outside the urban area of Glasgow, UK. International Journal of Biometeorology 57, 521–533. doi:10.1007/s00484-012-0578-y

Krüger, T., Held, F., Hoechstetter, S., 2014. Identifikation von hitzesensitiven Stadtquartieren. - In: Wende, W.; Rößler, S.; Krüger, T. (eds.), 2014. Grundlagen für eine klimawandel-angepasste Stadt- und Freiraumplanung, REGKLAM-Publikationsreihe, Heft 6. Rhombos-Verlag, Berlin. ISBN: 978-3-944101-15-6.

Kuttler, W., 2011. Climate change in urban areas. Part 2, Measures. Environmental Sciences Europe 23, 1-15.

Landeshauptstadt München, 2016. Indikatorenatlas. Available from: http://www.mstatistik-muenchen.de/indikatorenatlas/atlas.html?indicator=i57&date=2015. Last accessed: 7/30/2016.

Lehmann, I., Mathey, J., Rößler, S., Bräuer, A., Goldberg, V., 2014. Urban vegetation structure types as a methodological approach for identifying ecosystem services – Application to the analysis of micro-climatic effects. Ecological Indicators 42, 58–72. doi:10.1016/j.ecolind.2014.02.036

Lindberg, F., Grimmond, C.S.B., 2011. The influence of vegetation and building morphology on shadow patterns and mean radiant temperatures in urban areas: model development and evaluation. Theoretical and Applied Climatology 105, 311–323. doi:10.1007/s00704-010-0382-8

Lindberg, F., Onomura, S., Grimmond, C.S.B., 2016a. Influence of ground surface characteristics on the mean radiant temperature in urban areas. International Journal of Biometeorology. doi:10.1007/s00484-016-1135-x

Lindberg, F., Thorsson, S., Rayner, D., Lau, K., 2016b. The impact of urban planning strategies on heat stress in a climate change perspective. Sustainable Cities and Society. doi:10.1016/j.scs.2016.04.004

Lindley, S., O'Neill, J., Kandeh, J., Lawson, N., Christian, R., O'Neill, M., 2011. Climate change, justice and vulnerability. Joseph Rowntree Foundation, York.

Lissner, T.K., Holsten, A., Walther, C., Kropp, J.P., 2012. Towards sectoral and standardised vulnerability assessments: the example of heatwave impacts on human health. Climatic Change 112, 687–708. doi:10.1007/s10584-011-0231-5

Loughnan, M.E., National Climate Change Adaptation Research Facility (Australia), Monash University, 2013. A spatial vulnerability analysis of urban populations during extreme heat events in Australian capital cities.

Matzarakis, A., Mayer, H., 2000. Atmospheric conditions and human thermal comfort in urban areas, in: 11th Seminar on Environmental Protection, Environment and Health, Thessaloniki, Greece. pp. 153–166.

Matzarakis, A., Rutz, F., Mayer, H., 2010. Modelling radiation fluxes in simple and complex environments: basics of the RayMan model. International Journal of Biometeorology 54, 131–139. doi:10.1007/s00484-009-0261-0

Mayer, H., 1993. Urban bioclimatology. Experientia 49, 957–963.

McPherson, E.G., van Doorn, N., de Goede, J., 2016. Structure, function and value of street trees in California, USA. Urban Forestry & Urban Greening 17, 104–115. doi:10.1016/j.ufug.2016.03.013

McPherson, G.E., Nowak, D.J., Rowntree, R.A., 1994. Chicago's urban forest ecosystem: results of the Chicago Urban Forest Climate Project.

Meier, F., Scherer, D., 2012. Spatial and temporal variability of urban tree canopy temperature during summer 2010 in Berlin, Germany. Theoretical and Applied Climatology 110, 373–384. doi:10.1007/s00704-012-0631-0

Meteorologisches Institut München (MIM), 2016. Klimatabellen München, 1982-2016. Fachbereich Physik der Ludwigs-Maximilian Universität. Available from: http://www.meteo.physik.uni-muenchen.de/~paul.james/. Last accessed: 6/11/2016.

Moseley, D., Marzano, M., Chetcuti, J., Watts, K., 2013. Green networks for people: Application of a functional approach to support the planning and management of greenspace. Landscape and Urban Planning 116, 1–12. doi:10.1016/j.landurbplan.2013.04.004

Musy, M., Malys, L., Morille, B., Inard, C., 2015. The use of SOLENE-microclimat model to assess adaptation strategies at the district scale. Urban Climate 14, 213–223. doi:10.1016/j.uclim.2015.07.004

Nadim, F., 2013. Mitigation, in: Encyclopedia of Natural Hazards, Encyclopedia of Earth Sciences Series. Springer Netherlands, Dordrecht, pp. 682–683.

Natural England, 2009. Green Infrastructure Guidance.

Norton, B.A., Coutts, A.M., Livesley, S.J., Harris, R.J., Hunter, A.M., Williams, N.S.G., 2015. Planning for cooler cities: A framework to prioritise green infrastructure to mitigate high temperatures in urban landscapes. Landscape and Urban Planning 134, 127–138. doi:10.1016/j.landurbplan.2014.10.018

Oke, T.R., 1988. Street design and urban canopy layer climate. Energy and Buildings 11, 103–113. doi:10.1016/0378-7788(88)90026-6

Oliveira, S., Andrade, H., Vaz, T., 2011. The cooling effect of green spaces as a contribution to the mitigation of urban heat: A case study in Lisbon. Building and Environment 46, 2186–2194. doi:10.1016/j.buildenv.2011.04.034

Onomura, S., Grimmond, C.S.B., Lindberg, F., Holmer, B., Thorsson, S., 2015. Meteorological forcing data for urban outdoor thermal comfort models from a coupled convective boundary layer and surface energy balance scheme. Urban Climate 11, 1–23. doi:10.1016/j.uclim.2014.11.001

Portal München, 2016a. Bevölkerung. Daten zur Demografie. Available from: https://www.muenchen.de/rathaus/Stadtinfos/Statistik/Bev-lkerung.html. Last accessed: 8/26/2016.

Portal München, 2016b. Maxvorstadt. Available from: http://www.muenchen.de/stadtteile/maxvorstadt.html. Last accessed: 7/6/2016.

Portal München, 2016c. Branchenbuch München. Available from: http://www.muenchen.de/branchenbuch. Last accessed: 8/11/2016.

Raven, J., 2010. Cooling the Public Realm: Climate-Resilient Urban Design. - In: Otto-Zimmerman, K. (ed). Resilient Cities: Cities and Adaptation to Climate Change Proceedings of the Global Forum 2010. Local Sustainability 1. Springer, Dordrecht, pp. 451-465.

Reindl, D.T., Beckman, W.A., Duffie, J.A., 1990. Diffuse fraction correlations. Sol. Energy 45, 1–7. http://dx.doi.org/10.1016/0038-092X(91)90123-E.

Reid, C., O'Neill, M., Gronlund, C., Brines, S., Brown, D., Diez-Roux, A., Schwartz, J., 2009. Mapping Community Determinants of Heat Vulnerability. Environmental Health Perspectives. doi:10.1289/ehp.0900683

Reid, C.E., Mann, J.K., Alfasso, R., English, P.B., King, G.C., Lincoln, R.A., Margolis, H.G., Rubado, D.J., Sabato, J.E., West, N.L., Woods, B., Navarro, K.M., Balmes, J.R., 2012. Evaluation of a Heat Vulnerability Index on Abnormally Hot Days: An Environmental Public Health Tracking Study. Environmental Health Perspectives 120, 715–720. doi:10.1289/ehp.1103766

Romero-Lankao, P., Qin, H., Dickinson, K., 2012. Urban vulnerability to temperature-related hazards: A meta-analysis and meta-knowledge approach. Global Environmental Change 22, 670–683. doi:10.1016/j.gloenvcha.2012.04.002

Sarkar, C., Webster, C., Pryor, M., Tang, D., Melbourne, S., Zhang, X., Jianzheng, L., 2015. Exploring associations between urban green, street design and walking: Results from the Greater London boroughs. Landscape and Urban Planning 143, 112–125. doi:10.1016/j.landurbplan.2015.06.013

Scherber, K., Langner, M., Endlicher, W., 2014. Spatial analysis of hospital admissions for respiratory diseases during summer months in Berlin taking bioclimatic and socio-economic aspects into account. doi:10.12854/erde-144-16

Shashua-Bar, L., Hoffman, M.E., 2000. Vegetation as a climatic component in the design of an urban street: An empirical model for predicting the cooling effect of urban green areas with trees. Energy and Buildings 31, 221–235.

Sinnett, D., Smith, N., Burgess, S., 2015. Handbook on green infrastructure: planning, design and implementation. Edward Elgar Publishing Limited, Cheltenham, UK.

Spronken-Smith, R.A., Oke, T.R., 1999. Scale modelling of nocturnal cooling in urban parks. Boundary-Layer Meteorology 93, 287–312.

ten Brink, P., Mutafoglu, K, Kettunen, M., Twigger-Ross, C., Baker, J., Kuipers, Y, Emonts, M., Tyrväinen, L., Hujala, T., Ojala, A., 2006. The Health and Social Benefits of Nature and Biodiversity Protection. A report for the European Commission (ENV.B.3/ETU/2014/ 0039). Institute for European Environmental Policy, London; Brussels.

Thorsson, S., Rocklöv, J., Konarska, J., Lindberg, F., Holmer, B., Dousset, B., Rayner, D., 2014. Mean radiant temperature – A predictor of heat related mortality. Urban Climate 10, 332–345. doi:10.1016/j.uclim.2014.01.004

Tomlinson, C.J., Chapman, L., Thornes, J.E., Baker, C.J., 2011. Including the urban heat island in spatial heat health risk assessment strategies: a case study for Birmingham, UK. International journal of health geographics 10, 1.

Uejio, C.K., Wilhelmi, O.V., Golden, J.S., Mills, D.M., Gulino, S.P., Samenow, J.P., 2011. Intra-urban societal vulnerability to extreme heat: The role of heat exposure and the built environment, socioeconomics, and neighborhood stability. Health & Place 17, 498–507. doi:10.1016/j.healthplace.2010.12.005

Wang, Y., Akbari, H., 2016. Analysis of urban heat island phenomenon and mitigation solutions evaluation for Montreal. Sustainable Cities and Society 26, 438–446. doi:10.1016/j.scs.2016.04.015

Wilhelmi, O.V., Hayden, M.H., 2010. Connecting people and place: a new framework for reducing urban vulnerability to extreme heat. Environmental Research Letters 5, 14021. doi:10.1088/1748-9326/5/1/014021

Wilhelmi, O.V., Purvis, K.L., Harriss, R.C., 2004. Designing a geospatial information infrastructure for mitigation of heat wave hazards in urban areas. Natural Hazards Review 5, 147–158.

Wolf, T., McGregor, G., 2013. The development of a heat wave vulnerability index for London, United Kingdom. Weather and Climate Extremes 1, 59–68. doi:10.1016/j.wace.2013.07.004

Wolf, T., McGregor, G., Paldy, A., 2011. Integrated Assessment of Vulnerability to Heat Stress in Urban Areas, in: Brauch, H.G., Oswald Spring, Ú., Mesjasz, C., Grin, J., Kameri-Mbote, P., Chourou, B., Dunay, P., Birkmann, J. (Eds.), Coping with Global Environmental Change, Disasters and Security. Springer Berlin Heidelberg, Berlin, Heidelberg, pp. 1091–1099.

Wong, N.H., Kwang Tan, A.Y., Chen, Y., Sekar, K., Tan, P.Y., Chan, D., Chiang, K., Wong, N.C., 2010. Thermal evaluation of vertical greenery systems for building walls. Building and Environment 45, 663–672. doi:10.1016/j.buildenv.2009.08.005

Yu, B., Liu, H., Wu, J., Lin, W.-M., 2009. Investigating impacts of urban morphology on spatio-temporal variations of solar radiation with airborne LIDAR data and a solar flux model: a case study of downtown Houston. International Journal of Remote Sensing 30, 4359–4385. doi:10.1080/01431160802555846

Yu, C., Hien, W.N., 2006. Thermal benefits of city parks. Energy and Buildings 38, 105–120. doi:10.1016/j.enbuild.2005.04.003

Appendix

Table 5: Overview of heat vulnerability indexes with authors, location, indicators and aggregation methods. PCA= principal component analysis (Source: Bao et al., 2015, pp.7223f; Chuang 2013, pp. 40f; own additions)

Author (Time, Location)	Indicator (Numbers)	Methods
Vescovi et al. (2005, Southern Quebec)	hot days, consecutive hot days with Tmax > 30°C and Tmin > 22°C, elderly, poverty, isolation, education (6)	normalization, equal weight
Lindley (2006, Greater London)	maximum temperature, elderly and living alone, very young (<4y), chronic illnesses, mental health problems or bedridden, income disparity, land use type (7)	
Reid et al. (2009, USA)	poverty, education, living alone, ethnicity, population above 65 yrs. old, population above 65 yrs. old and living alone, vegetation, diabetes, central AC, AC of any kind (10)	PCA
Rinner et al. (2010, Toronto)	land surface temperature, vegetation, old dwelling without AC, high-density dwellings without AC, behavior, illness, cognitive impairment, elderly, infants and young children, poverty, rental households, isolation, homeless, education, not English speaking, recent immigrants, ethnicity, home cooling, drop-in centers, participating community outreach centers, cooling centers (21)	ordered weighted averaging, local indicators of spatial association
Hondula et al. (2012, Philadelphia)	surface temperature (2004 and 2008), low/mid/high density residential, recreational, industrial, mixed use land, commercial, building coverage, White, Black, American Indian, Asian, Pacific Islander, other race, two or more races, nonwhite, elderly, education, income, below poverty line, below 2x poverty line, aged people living alone, living alone(25)	PCA, multiple linear regression
Chow et al. (2012, Phoenix)	mean summer maximum/minimum temperature, mean normalized difference vegetation index, elderly, income, foreign-born noncitizens, immigrants (7)	normalization, equal weight
Johnson et al. (2012, Chicago)	land surface temperature, elderly women, elderly men, lonely elderly women, white population, female heads of household, lonely elderly men, family income, per capita income, household income, population with less than high school education, Asian population, population aged 65 and older in group living, other race population, Hispanic population, population 25 and older with a high school education, built-up index, vegetation index, black population (19)	PCA
Loughnan et al. (2012, Melbourne)	aged care facilities, ethnicity, aged people living alone, infants and elderly, urban density (5)	regression analysis, weighting of indicators according to their contribution

Tomlinson et al. (2012, Birmingham)	land surface temperature, elderly, ill, density of households, flat (5)	normalization, equal weight
Depietri et al. (2013, Cologne)	land surface temperature, land use, land cover, forest cover, number of inhabitants, unemployed, elderly living alone (7)	multi-criteria outranking approach
Wolf et al. (2013, London)	land surface temperature, households in rented tenure, flat, population density, households without central heating, elderly, self-report bad health status, receiving social benefit, single pensioner households, ethnicity (10)	PCA, spatial clustering
Aubrecht et al. (2013, U.S. National Capital Region)	heat wave day count, elderly, living alone, poverty, poor English skills, education, vegetation (7)	normalization, equal weight
Maier et al. (2013, Georgia)	poverty, education, ethnicity, living alone, elderly, elderly and living alone, diabetes, land use (8)	PCA
Chuang (2013)	poverty, low education level, central AC, AC of any kind, living alone, ethnicity, elderly, elderly living alone, diabetes, density of green space (10)	PCA
Harlan et al. (2013, Maricopa county)	ethnicity, immigrant, poverty, education, central AC, elderly, elderly and living alone, living alone, unvegetated area (mean), unvegetated area (SD), surface temperature (11)	PCA, local indicators of spatial association
Dong et al. (2014, Beijing)	heat wave days, extremely high temperature days, population density, elderly ratio, income level, land use/cover (6)	normalization, equal weight
Dugord et al. (2014, Berlin)	air temperature, population density, concentration of vulnerable inhabitants (high or low age)	weighting by population density
Zhu et al. (2014, Guangdong)	elderly, infant, immigrant, unemployment, agricultural population, infant mortality rate, health worker, GDP per capita, living space, harmless sanitary latrines, illiteracy rate, temperature growth, heat wave day count (13)	analytic hierarchy process, principal component analysis
El-Zein et al. (2015, Sydney)	maximum temperature, minimum temperature, high temperature days, land cover, population density, road density, elderly, elderly and living alone, children, multiunit dwellings, population completing year 12, not English speaking, home loan repayment, home ownership, household income, internet access, assets to liabilities of local council, business rates, residential rates, community service expenses, environmental and health expenses, population requiring financial assistance (22)	multi-criteria outranking approach
Norton et al., 2015 (Melbourne)	daytime and nighttime temperature, elderly, young (<5 y), socio-economic disadvantaged, population behavioral exposure (6)	normalization, equal weight

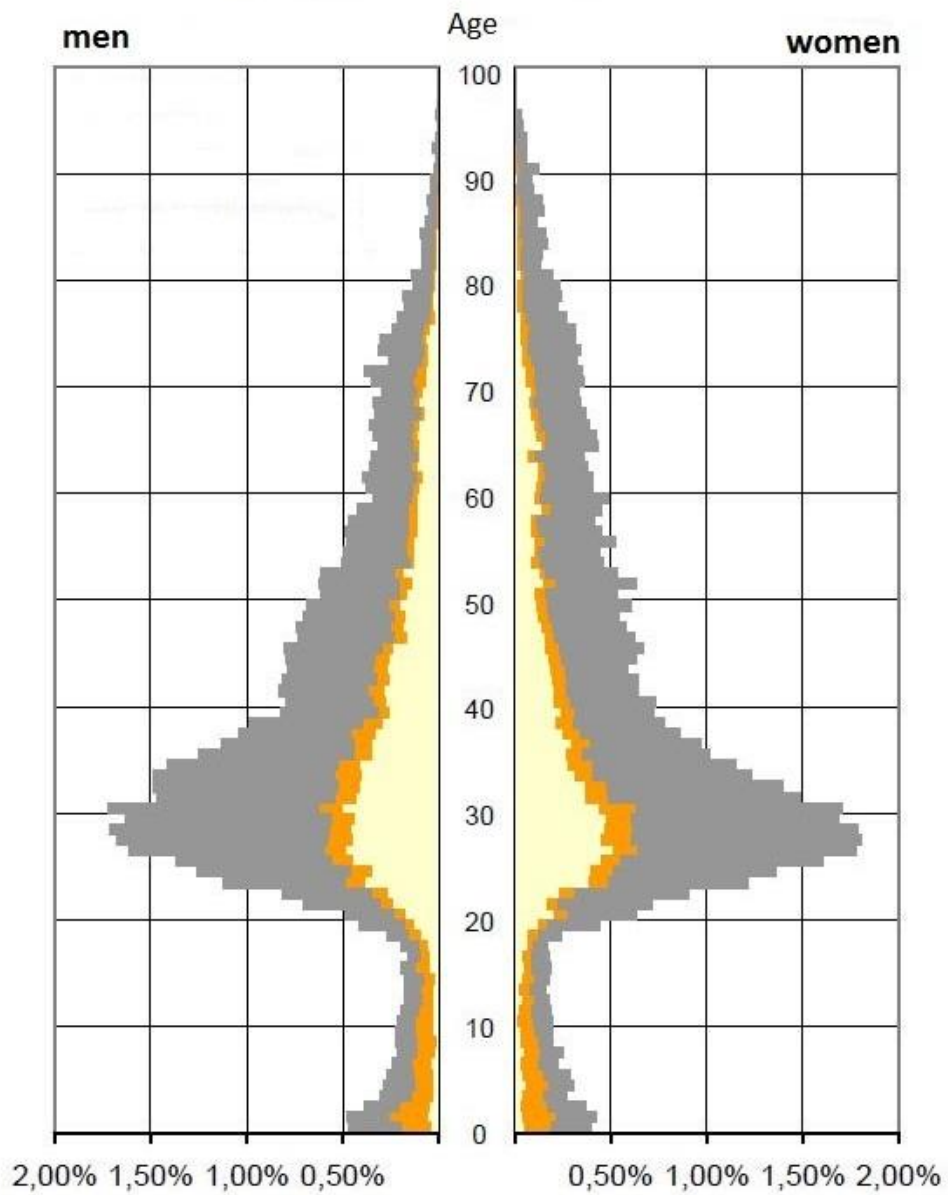*Figure 28: Distribution of the residents' age for Maxvorstadt on 31st December 2014. yellow= foreigners, grey: Germans, orange= Germans with migration background (Source: Statistisches Taschenbuch 2015, p.31, adapted)*

	Jan	Feb	Mar	Apr	May	Jun	Jul	Aug	Sep	Oct	Nov	Dec	Ann
2016	0	0	0										
2015	0	0	0	0	0	1	16	17	3	0	0	0	37
2014	0	0	0	0	1	5	3	1	0	0	0	0	10
2013	0	0	0	0	0	4	12	8	0	0	0	0	24
2012	0	0	0	1	1	4	2	5	0	0	0	0	13
2011	0	0	0	0	0	0	0	8	1	0	0	0	9
2010	0	0	0	0	0	2	12	2	0	0	0	0	16
2009	0	0	0	0	2	1	3	5	1	0	0	0	12
2008	0	0	0	0	4	4	6	2	0	0	0	0	16
2007	0	0	0	0	3	1	7	2	0	0	0	0	13
2006	0	0	0	0	0	7	18	0	1	0	0	0	26
2005	0	0	0	0	2	5	5	0	0	0	0	0	12
2004	0	0	0	0	0	1	0	1	0	0	0	0	2
2003	0	0	0	0	2	6	5	12	0	0	0	0	25
2002	0	0	0	0	0	6	1	0	0	0	0	0	7
2001	0	0	0	0	0	1	3	4	0	0	0	0	8
2000	0	0	0	0	0	4	0	3	0	0	0	0	7
1999	0	0	0	0	0	0	3	0	0	0	0	0	3
1998	0	0	0	0	0	3	3	3	0	0	0	0	9
1997	0	0	0	0	0	0	0	0	0	0	0	0	0
1996	0	0	0	0	0	2	1	0	0	0	0	0	3
1995	0	0	0	0	0	0	3	0	0	0	0	0	3
1994	0	0	0	0	0	4	7	4	0	0	0	0	15
1993	0	0	0	0	1	0	0	1	1	0	0	0	3
1992	0	0	0	0	0	0	3	12	0	0	0	0	15
1991	0	0	0	0	0	0	2	1	0	0	0	0	3
1990	0	0	0	0	0	0	1	3	0	0	0	0	4
1989	0	0	0	0	0	0	0	2	0	0	0	0	2
1988	0	0	0	0	0	0	2	2	0	0	0	0	4
1987	0	0	0	0	0	1	0	0	0	0	0	0	1
1986	0	0	0	0	0	0	0	2	0	0	0	0	2
1985	0	0	0	0	0	0	4	2	0	0	0	0	6
1984	0	0	0	0	0	0	3	0	0	0	0	0	3
1983	0	0	0	0	0	0	8	1	1	0	0	0	10
1982	0	0	0	0	0	0	3	1	0	0	0	0	4
Mean	0.0	0.0	0.0	0.0	0.5	1.8	4.0	3.1	0.2	0.0	0.0	0.0	9.6
Trend	0.0	0.0	0.0	0.0	0.4	1.2	1.8	1.5	0.2	0.0	0.0	0.0	5.1
	Jan	Feb	Mar	Apr	May	Jun	Jul	Aug	Sep	Oct	Nov	Dec	Ann

Figure 29: Number of heat days (T_{air} > 30°C) at weather station Theresienstraße from 1982-2016 (Source: Meteorologisches Institut München (MIM), 2016)

Table 6: Statistics for Maxvorstadt's urban structure types (Data source: ZSK, 2013)

| No.	name	count	vegetation (%)	sealed (%)	buildings (%)	total area (ha)	%of total area
1	service roads	52	-	100	0	59	14.7
2	perimeter buildings	129	22.6	84.5	64.1	179	44.6
3	perimeter development	2	31.2	68.8	59.7	0.3	0.1
4	mixed development	2	59.3	75.8	48.7	4.3	1.1
5	track installations	1	-	-	0	0.3	0.1
6	large construction sites	1	28.8	71.2	51.5	1.3	0.3
7	large avenues	5	90	10	0.6	1.5	0.4
8	large storey buildings	25	32.3	68.8	48.2	51	12.8
9	big parking lots	1	28.2	71.8	63.7	1	0.2
10	main roads	18	-	100	0	34	8.5
11	chain buildings	1	42	58	36.9	2	0.5
12	small storey buildings	6	35.7	64.3	42.6	7.6	1.9
13	small green areas	20	83.7	29.8	0.1	8	2
14	small detached buildings	4	34.8	63.8	44.6	3.2	0.8
15	large mixed development	5	8.2	91.8	57.4	14.3	3.6
16	public places	5	28.7	71.3	0.3	0.4	0.1
17	parks	7	96.2	6.6	2.2	17	4.3
18	high rise buildings	6	61.1	38.9	27.5	6.5	1.6
19	special constructions	6	37.6	62.4	38.8	5	1.2
20	linear development	3	40.2	59.8	52.8	5	1.2
	Maxvorstadt total	300	25	80	41	401	100
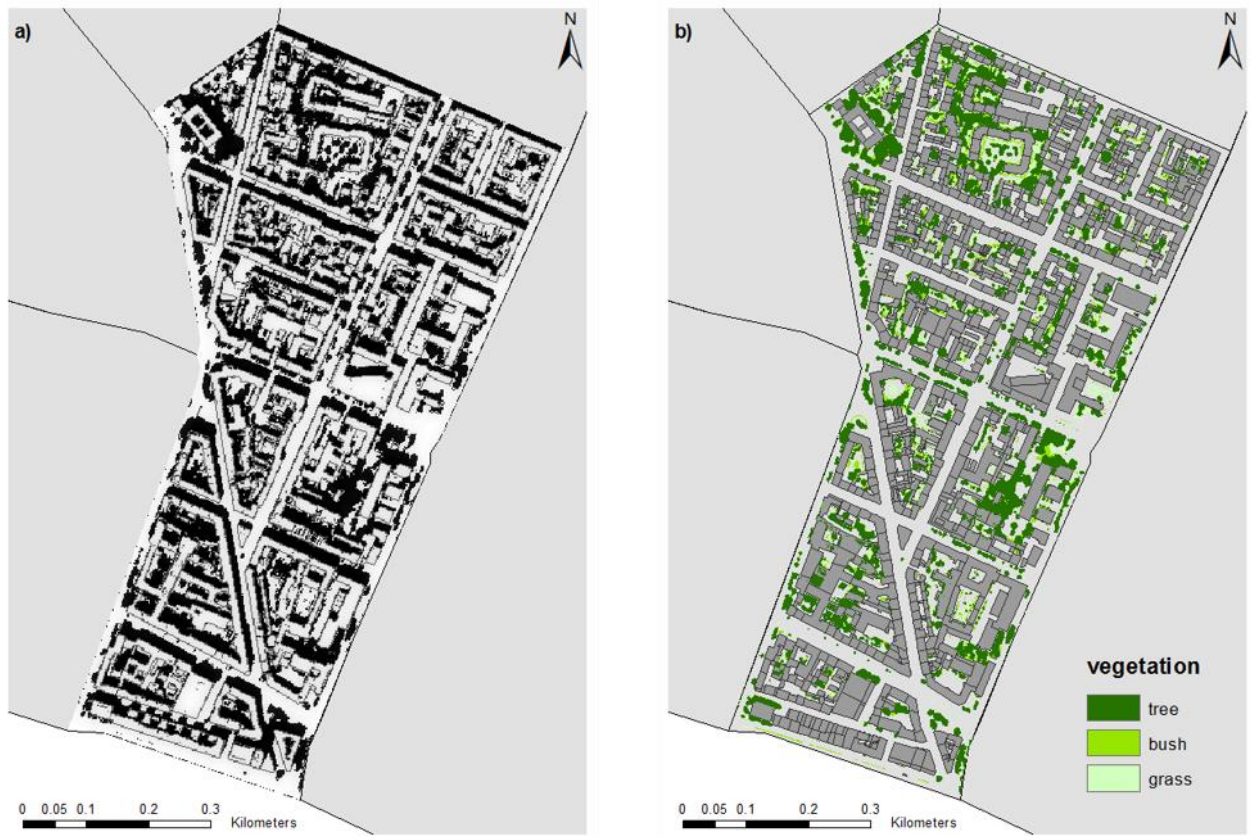
Figure 30: CDP Augustenstraße: groundviewfactor (a) and vegetation coverage (b)

Eidesstattliche Erklärung

Familienname: Erlwein
Vorname: Sabrina
Geburtsdatum: 09.10.1990

Ich erkläre hiermit an Eides statt, dass ich die vorliegende Arbeit eigenständig ohne unzulässige Hilfe Dritter und ohne Benutzung anderer als der angegebenen Hilfsmittel angefertigt habe. Die aus anderen Quellen direkt oder indirekt übernommenen Daten und Konzepte sind unter Angabe des Literaturzitats gekennzeichnet. Das gilt auch für Zeichnungen, Skizzen, bildliche Darstellungen und dergleichen sowie für Quellen aus dem Internet und unveröffentlichte Quellen.

Die Arbeit wurde bisher weder im In- noch im Ausland in gleicher oder ähnlicher Form einer anderen Prüfungsbehörde vorgelegt und war bisher nicht Bestandteil einer Studien- oder Prüfungsleistung.

_____   _____
       (Ort, Datum)   (Unterschrift)